Atmospheric
Chemistry
and Physics
Discussions

Open Access

Reactive uptake of ammonia to secondary organic aerosols: kinetics of organonitrogen formation

Y. Liu[1,2], J. Liggio[1], R. Staebler[1], and S.-M. Li[1]

[1]Atmospheric Science and Technology Directorate, Science and Technology Branch, Environment Canada, Toronto, M3H 5T4, Canada
[2]State Key Joint Laboratory of Environment Simulation and Pollution Control, Research Center for Eco-Environmental Sciences, Chinese Academy of Sciences, Beijing, 100085, China

Correspondence to: J. Liggio (john.liggio@ec.gc.ca)

Discussion Paper | **Discussion Paper** | **Discussion Paper** | **Discussion Paper**

ACPD

15, 17449–17490, 2015

Reactive uptake of ammonia to secondary organic aerosols

Y. Liu et al.

Title Page

Abstract	Introduction
Conclusions	References
Tables	Figures

|◄ | ►|
◄ | ►
Back | Close

Full Screen / Esc

Printer-friendly Version

Interactive Discussion

Abstract

As a class of brown carbon, organonitrogen compounds originating from the heterogeneous uptake of NH_3 by secondary organic aerosol (SOA) have received significant attention recently. In the current work, particulate organonitrogen formation during the ozonolysis of α-pinene and the OH oxidation of m-xylene in the presence of ammonia (34–125 ppb) is studied in a smog chamber equipped with a High Resolution Time-of-Flight Aerosol Mass Spectrometer and a Quantum Cascade Laser instrument. A large diversity of nitrogen containing organic (NOC) fragments was observed which were consistent with the reaction of ammonia with carbonyl containing SOA. The uptake coefficients of NH_3 to SOA leading to organonitrogen compounds are reported for the first time and were in the range of $\sim 10^{-3}$–10^{-2}, decreasing significantly to $< 10^{-5}$ after 6 h of reaction. At the end of experiments (~ 6 h) the NOC mass contributed 8.9 ± 1.7 and 31.5 ± 4.4 wt% to the total α–pinene and m-xylene derived SOA, and 4–15 wt% of the total nitrogen in the system. Uptake coefficients were also found to be positively correlated with particle acidity and negatively correlated with NH_3 concentration, indicating that heterogeneous reactions were responsible for the observed NOC mass, possibly limited by liquid phase diffusion. Under these conditions, the data also indicate that the formation of NOC can compete kinetically with inorganic acid neutralization. The formation of NOC in this study suggests that a significant portion of the ambient particle associated N may be derived from NH_3 heterogeneous reactions with SOA. NOC from such a mechanism may be an important and unaccounted for source of PM associated nitrogen, and a mechanism for medium or long-range transport and dry/wet deposition of atmospheric nitrogen.

Title Page

Abstract	Introduction
Conclusions	References
Tables	Figures

|◄ | ►|

◄ | ►

Back | Close

Full Screen / Esc

Printer-friendly Version

Interactive Discussion

1 Introduction

Black carbon (BC) and brown carbon (BrC) are the most abundant and effective light absorbing components in atmospheric particles (Stocker et al., 2013; Andreae and Gelencser, 2006). While BC has been extensively studied (Cappa et al., 2012; Bond et al., 2013), BrC is currently receiving significant attention from the atmospheric chemistry community as it is often more abundant than BC in the atmosphere (Powelson et al., 2014), and has the potential to be an important climate forcing agent via direct absorption of light (Alexander et al., 2008). BrC refers to organic matter in atmospheric particles that absorb light with a strong wavelength dependence (Andreae and Gelencser, 2006; Powelson et al., 2014; Alexander et al., 2008). It exists in various forms, such as soil derived humic materials, humic-like substances (HULIS), organic materials from combustion processes, bioaerosols (Andreae and Gelencser, 2006; Salma et al., 2010) and secondary formation in the atmosphere (Updyke et al., 2012; Zarzana et al., 2012; Nguyen et al., 2013; Powelson et al., 2014). Although the chemical composition of BrC is highly complex, light absorption by BrC in the ultraviolet-visible region, quantified by the mass absorption coefficient (MAC) (typically in the range of 0.001– 0.1 $m^2 g^{-1}$ at 500 nm of wavelength; Updyke et al., 2012), is ascribed to the π-π^* and n-π^* bond transitions of electrons in the chemicals present. The π-π^* transition is usually observed in species with unsaturated bonds, while n-π^* transitions are relevant to heteroatoms coupled to unsaturated bonds.

Primary emissions of biomass burning particles are regarded as an important source of BrC (Saleh et al., 2013; Andreae and Gelencser, 2006) since polycyclic aromatic hydrocarbons (PAHs), nitro-PAHs, oxy-PAHs and other aromatic hydrocarbons, and therefore unsaturated bonds, are abundant in these combustion particles (Andrade-Eiroa et al., 2010; Kinsey et al., 2011; Souza et al., 2014). Secondary formation of particulate organics have also recently been considered another significant source of BrC through heterogeneous or multiphase chemical reactions (Updyke et al., 2012; Zarzana et al., 2012; Nguyen et al., 2013; Powelson et al., 2014), in which heteroatoms

including O, S, and N can be introduced into the particulate matter via a variety of precursors. For example, as characteristic components of HULIS (Nguyen et al., 2014, 2012), organosulfates and organonitrates have been observed in both laboratory generated (Liggio and Li, 2006b; Iinuma et al., 2009; Russell et al., 2011; Darer et al., 2011) and ambient organic particles (Hawkins et al., 2010; Surratt et al., 2006; Russell et al., 2011). Oxygen and nitrogen-containing oligomers of high molecular weight have also been identified in secondary organic aerosols (SOA) (Kalberer et al., 2004).

N-containing organic compounds (NOC) are an important class of heteroatom containing BrC compounds and can account for an appreciable fraction of organic aerosol mass (Beddows et al., 2004; Cheng et al., 2006; Kourtchev et al., 2014) which has mainly been attributed to biomass burning and cooking emissions (Cheng et al., 2006). However, heterogeneous reactions are increasingly being considered an important source of particle bound organonitrogen compounds. For example, acid-base reactions between ammonia or amines and acid moieties (Liu et al., 2012b; Kuwata and Martin, 2012) or exchange reactions of amines with inorganic ammonium salts (Chan and Chan, 2012; Bzdek et al., 2010; Qiu et al., 2011; Liu et al., 2012a) can lead to the formation of particle bound ammonium salts. Schiff base and/or Mannich reactions between NH_3, ammonium salts or amines with carbonyl functional groups in particles can also form organonitrogen compounds, in which N atoms can be coupled to double bonds (imines) and act as effective chromophors since both π-π^* and n-π^* transitions are possible (Nguyen et al., 2013). It has also been proposed that Mannich reactions may be a possible formation mechanism for the high-molecular weight nitrogen-containing organic species observed in ambient particles (X. F. Wang et al., 2010). In laboratory studies, the formation of light absorbing compounds has been inferred by a significant enhancement in visible light absorption during reactions between glyoxal/methylgloxyal and primary amines glycine, methylamine and ammonium (Zarzana et al., 2012; Yu et al., 2011; Powelson et al., 2014; Lee, A. K. Y. et al., 2013; Trainic et al., 2011) as well as between O_3/OH initiated biogenic and anthropogenic SOA and NH_3 (Updyke et al., 2012; Nguyen et al., 2013; Lee, H. J. et al., 2013; Bones et al., 2010). Using High

Resolution Time-of-Flight Aerosol Mass Spectrometry (HR-ToF-AMS) and Desorption Electrospray Ionization Mass Specetrometry (DESI-MS), characteristic fragments containing nitrogen ($C_xH_yN_n$ and $C_xH_yO_zN_n$) from the above reactions have been identified (Galloway et al., 2009; Laskin et al., 2010; Lee, A. K. Y. et al., 2013).

5　　In addition to the noted role of organonitrogen in BrC, heterogeneously formed organonitrogen may be an important nutrient to ecosystems via nitrogen (N) deposition from the atmosphere (Liu et al., 2013). Heterogeneous reactions leading to NOC can be considered a process whereby gas-phase nitrogen compounds such as NH_3 or amines with short lifetimes (via deposition) (Liggio et al., 2011) are transformed to

10　particle-phase nitrogen compounds with increased atmospheric lifetimes. The subsequent transport and deposition of particle-phase organonitrogen compounds (rather than gas-phase N) may have an impact on regional nitrogen cycles by altering N deposition patterns. However, this process has generally not been considered in current deposition models (García-Gómez et al., 2014) due to limited knowledge on the forma-

15　tion kinetics and mechanisms of NOC formation from heterogeneous reactions.

　　While reactions of amines have been implicated as a source of particulate-phase reduced nitrogen (Zarzana et al., 2012), their ambient gaseous concentrations are typically low (Cornell et al., 2003). NH_3 is the most abundant form of gas-phase reduced nitrogen in the atmosphere with global emissions estimated at greater than $33\,\mathrm{Tg}\,(\mathrm{N})\,\mathrm{yr}^{-1}$

20　(Reis et al., 2009) and typical ambient concentration of several ppbv (Cornell et al., 2003; Heald et al., 2012). As qualitatively confirmed by mass spectrometry in various experiments (Updyke et al., 2012; Nguyen et al., 2013; Lee, H. J. et al., 2013; Bones et al., 2010), reactions between NH_3 and OA are possible in the atmosphere leading to particulate reduced nitrogen. In order to assess and model the impacts of the Schiff

25　base, Mannich or other NOC forming reactions (via NH_3) on the radiative forcing potentials of ambient SOA and N-deposition, the kinetics of such reactions are required, and yet they remain largely unknown. To the best of our knowledge, there is only one paper which reported the formation rate constant of imidazole-2-caroxaldehyde (IC) to be

Title Page

Abstract	Introduction
Conclusions	References
Tables	Figures

◄ | ►◄

◄ | ►

Back | Close

Full Screen / Esc

Printer-friendly Version

Interactive Discussion

$(2.01 \pm 0.40) \times 10^{-12} \, M^{-2} \, s^{-1}$ for the reaction between glyoxal and aqueous $(NH_4)_2SO_4$ in an effort to simulate cloud processing (Yu et al., 2011).

In the current study, heterogeneous reactive uptake coefficients (γ) for NH_3 on laboratory SOA, which lead to the formation of particulate NOC, were derived using a smog chamber coupled to a HR-ToF-AMS. The influence of VOC precursors, seed particle acidity/composition and gaseous NH_3 concentration on the obtained uptake coefficients of NH_3 is also investigated. Finally, the implications of the kinetics on atmospheric BrC and N-deposition are also discussed.

2 Experimental details

2.1 Chamber experiments

Experiments were performed in a $9 \, m^3$ cylindrical smog chamber, which has been described in detail by Bunce et al. (Bunce et al., 1997). Briefly, this reactor is constructed with 50 μm FEP Teflon film and housed in an air-conditioned room ($295 \pm 2 \, K$). The surface-to-volume (S/V) ratio is $2.7 \, m^{-1}$. Twenty four black light lamps (Sylvania, F40/350BL) were installed outside the reactor for photochemical reactions. Before each experiment, the chamber was cleaned by irradiation (300–400 nm, 350 nm peak wavelength) for 8 h followed by continuous flushing with zero air for 24 h, after which the concentration of particles and ammonia was $< 1 \, particle \, cm^{-3}$ and $\sim 5 \, ppbv$, respectively.

A summary of initial experimental conditions is given in Table 1. Na_2SO_4/H_2SO_4 particles were generated as seeds via atomization (model 3706, TSI), dried through a diffusion drier, and size-selected with a differential mobility analyzer (DMA) (model, 3081, TSI) to have a mode mobility diameter (D_m) of $\sim 90 \, nm$. A high concentration of Na_2SO_4/H_2SO_4 seeds ($\sim 5000 \, particle \, cm^{-3}$) was added into the chamber to suppress new particle formation from the added VOC precursor and oxidant. As shown in Fig. S2, new particle formation was suppressed during subsequent SOA formation. α-pinene

or m-xylene (Sigma Aldrich) were added into the chamber via a syringe which was purged with zero air prior to use. The VOC concentrations were measured online with a High Resolution Time-of-Flight Proton Transfer Reaction Mass Spectrometry (HR-ToF-PTRMS, Ionic Analytic). SOA was formed via the oxidation of the VOCs by O_3
or OH. The concentration, size and composition of SOA coated on the seed particles were measured with a Scanning Mobility Particle Sizer (SPMS, TSI) and a HR-ToF-AMS (Aerodyne) (DeCarlo et al., 2006) operated alternately in both V- and W-mode. HR-ToF-AMS data were analyzed with the software PIKA 1.12 (DeCarlo et al., 2006; Aiken et al., 2007). The concentration of NOC was determined by fitting peaks including
those from the NH_x, NO_x, $C_xH_yN_n$, $C_xH_yON_n$ and $C_xH_yO_2N_n$ fragment groups. Particle wall loss was accounted for by normalizing SOA and NOC concentrations to the sulfate seed signal from the HR-ToF-AMS. It should be noted that the NOC concentration may be underestimated in this study since one cannot resolve all the nitrogen containing fragments that may exist, and since some of the NOCs may fragment into masses that
do not contain nitrogen and thus are quantified as organic. Furthermore, the relative ionization efficiency (RIE) for the NOC fragments was assumed to be equivalent to the remainder of the organics (1.4), since a RIE value for NOC is unknown. This may introduce an additional uncertainty to the quantitation of NOC.

O_3 was generated by passing zero air through an O_3 generator (OG-1, PCI Ozone
Corp.) and measured with an O_3 monitor (model 205, 2B Technologies). OH was produced by photolysis of H_2O_2 (Wang, K. et al., 2010; Donahue et al., 2012), which was added by bubbling zero air through a 30 % H_2O_2 solution (Sigma Aldrich). Details regarding the OH concentration determination and the oxidant levels during these experiments are described further in the supporting information (SI). NH_3 from a standard
cylinder was added into the chamber though a passivated mass flow controller. NH_3 concentration in the chamber was measured with a Quantum Cascade Laser (QCL, Aerodyne), whose principle of operation has been described elsewhere (Kosterev et al., 2002).

Unfortunately, the NH_3 background in the dry chamber was consistently at ~ 5 ppbv (after cleaning), increasing to a reproducible ~ 35 ppbv after humidifying to 50 % RH. While this limited the ability to perform experiments in the complete absence of ammonia, it did not preclude the derivation of kinetics at the lowest concentration (35 ppbv) and higher attained by further additions of ammonia. In some experiments, external NH_3 was added to the reactor after ~ 6 h of reaction to measure the uptake kinetics of NH_3 by relatively aged SOA. All experiments were conducted at 50 ± 2 % RH, with zero air provided by an AADCO-737 generator (AADCO Instruments Inc.).

The presence of NOC in the SOA particles was also confirmed by Fourier Transform Infrared (FTIR) Spectroscopy. SOA was collected on a silver membrane filter (0.2 μm, 47 mm, Sterlitech; stainless steel filter holder), which has a wide IR window in the range of 650–4000 cm^{-1}. A second filter placed behind the first one was used as a reference sample for IR measurements. The IR spectra were recorded with a mercury cadmium telluride (MCT) detector at a resolution of 4 cm^{-1} for 200 scans in Diffuse Reflectance Infrared Fourier Transform Spectroscopy (DRIFTS) mode, using an iS50 spectrometer (Nicolet).

2.2 Derivation of kinetics

Reactive uptake coefficients (γ) of NH_3 to form NOC were calculated based upon the measured concentration time series of nitrogen atom (N) mass derived from the HR-ToF-AMS fragment families of $C_xH_yN_n$, $C_xH_yON_n$, $C_xH_yO_2N_n$, NH_x and NO_x using an uptake model that has been described in detail previously (Liggio et al., 2005b; Liggio and Li, 2006a). Briefly, the change in the mass of N (within the NOC) added to a particle exposed to NH_3 as a function of time can be described by,

$$\frac{dm_N}{dt} = \gamma_{obs}\pi a^2 \langle c \rangle c_{NH_3} F_h \tag{1}$$

where a, $\langle c \rangle$ and c_{NH_3} are the particle radius, mean molecular speed, and gas-phase concentration of NH_3, respectively; γ_{obs} is the observed uptake coefficient of NH_3 to

form NOC (specifically the N in the NOC); F_h is a heterogeneous mass factor that accounts for the loss of hydrogen in ammonia as it reacts heterogeneously to form particulate phase NOC. We assume F_h is equal to 0.824 (i.e.: N/NH_3) in this study. From Eq. (1), the N mass as a function of time is given by:

$$m_N = \left(\frac{b\pi c_{NH_3}\langle c \rangle F_h(t-t_0)\gamma_{obs} + 3(bm_0 + d)^{1/3}}{3b^{1/3}} \right)^3 - \frac{d}{b} \tag{2}$$

where, $b = \frac{3}{4\pi\rho}$, $d = a_0^3$ and are constants. The uptake coefficient (γ) is derived from a fit of Eq. (2) to the experimental data. Further detail on the derivation and the parameters used in the fits is given in the SI. It should be pointed out that the NH_x^+ family (NH^+, NH_2^+ and NH_3^+) in the AMS mass spectra may be primarily associated with inorganic ammonium from the neutralization of the H_2SO_4 in the seed particle. However an unknown fraction of the NH_x^+ will arise from the fragmentation of NOC. For this reason, the uptake coefficients have been derived including and excluding the N mass of NH_x^+ as upper and lower bounds to γ.

3   Results and discussion

3.1   Identification of NOC

A typical mass spectrum of SOA from the ozonolysis of α-pinene between 4 and 6 h of reaction in the presence of 40.8 ppbv NH_3 (Exp. P6) is shown in Fig. 1. The spectrum is dominated by C_xH_y fragments at m/z 27 ($C_2H_3^+$), 39 ($C_3H_3^+$), 41($C_3H_5^+$) and 53 ($C_4H_7^+$); C_xH_yO fragments at m/z 28 (CO^+), 43 ($C_2H_3O^+$) and 55 ($C_3H_3O^+$); and $C_xH_yO_2$ fragments at m/z 44 (CO_2^+) and 45 (CHO_2^+). The presence of these fragment families and the overall mass spectrum is consistent with previously reported mass spectra of SOA formed from the O_3 oxidation of α-pinene at low SOA mass loading ($< 15\,\mu g\,m^{-3}$) (Shilling et al., 2009).

17457

In the presence of NH_3, a number of N-containing fragments are also observed. The mass spectrum containing N-containing fragments only is shown in Fig. 1b. Strong peaks belonging to the $C_xH_yN_n$ family of fragments dominate the spectrum at m/z 27 (CHN^+), 30 (CH_4N^+), 42 ($C_2H_4N^+$), 43 ($C_2H_5N^+$), 54 ($C_3H_4N^+$), 55 ($C_3H_5N^+$) and 68 ($C_3H_4N_2^+$, $C_4H_6N^+$). Less prevalent peaks from the $C_xH_yON_n$ and $C_xH_yO_2N_n$ group of fragments are also observed at m/z 44 (CH_2ON^+), 45 (CH_3ON^+), 58 ($C_2H_4ON^+$), 68 ($C_3H_2ON^+$), 73 ($C_2H_5ON_2^+$, $C_3H_7ON^+$), 86 ($C_3H_6ON_2^+$), 97 ($C_4H_5ON_2^+$), 73 ($C_3H_2O_2N^+$), 86 ($C_2H_2O_2N_2^+$), and 91 ($C_3H_9O_2N^+$). Although the signal intensities of N-containing fragments are weaker than those of the C_xH_y, C_xH_yO and $C_xH_yO_2$ families, the results demonstrate that N-containing species are formed.

Similar OA mass spectra were obtained from the OH oxidation ($H_2O_2 + h\nu$) of m-xylene (Fig. S3). As shown in Fig. S3, the relative intensities of C_xH_y, C_xH_yO and $C_xH_yO_2$ fragment families are slightly different than those of SOA formed via OH oxidation of m-xylene reported previously (Loza et al., 2012), which is likely due to differences in experimental reaction conditions such as the oxidant level and mass loading. The mass spectrum of N-containing fragments for m-xylene derived SOA are given in Fig. S3b, and are also somewhat different than those observed for α-pinene derived SOA (Fig. 1b). For example, the fragments at m/z 68 ($C_3H_4N_2^+$, $C_4H_6N^+$ and $C_3H_2ON^+$), 91 ($C_3H_9O_2N^+$) and 97 ($C_4H_5ON_2^+$) are significantly weaker in the SOA from m-xylene (Fig. S3b) than those from the ozonolysis of α-pinene (Fig. 1b), suggesting the presence of different types and quantities of the SOA functional groups required for the organonitrogen forming heterogeneous reactions.

The formation of NOC is further confirmed via the IR spectra of the SOA formed in the presence of NH_3. The IR spectra of SOA from the ozonolysis of α-pinene and the OH oxidation of m-xylene is shown in Fig. 2 and the assignments of the observed IR bands are summarized in Table S1 in the Supplement. After 6 h of ammonia exposure a number of nitrogen containing bands are tentatively identified. These include, NH_x (ν_{as,NH_2}: 3490; ν_{as,NH_3^+}: 3240 cm^{-1}; δ_{NH} or $\nu_{s,CN}$ 1563; and 785 or 740 cm^{-1}) and C=N ($\nu_{s,CN}$: 1640; $\nu_{s,CN}$: 1660 cm^{-1}) (Nguyen et al., 2013; Lin-Vien et al., 1991) functional

groups which are observable in the SOA from both α-pinene and m-xylene. The generally small IR signals associated with the NOC make it difficult to conclusively assign a number of potential NOC bands particularly since the expected dominant carbonyl and organic acid functional groups associated with SOA are also observed (Table S1).

5   While the above IR assignments are common between experiments using both VOC precursors, the OH oxidation of m-xylene resulted in a very strong band at 2195 cm^{-1}, which was not present in the α-pinene derived SOA (Fig. 2) and was assigned to $v_{s,C=C-C\equiv N}$ (Lin-Vien et al., 1991) (a nitrile). At the present time, the exact formation mechanism leading to this functional group is unknown. However, the double bond

10 adjacent to the nitrile group suggests that it is unique to the oxidative ring opening of m-xylene (and likely other aromatics), which is not accessible in the α-pinene system. Regardless, the functional groups revealed in the IR absorption spectra supports the HR-ToF-AMS results and confirms the formation of particle bound NOC.

3.2   Potential mechanisms contributing to observed NOC

15 Several mechanisms have been postulated previously with respect to NOC formation in the presence of ammonia. The various mechanisms generally fall into two categories: reactions of ammonia/ammonium with carbonyl functional groups in SOA leading to the formation of species with covalently bonded carbon to nitrogen (X. F. Wang et al., 2010; Zarzana et al., 2012; Yu et al., 2011; Powelson et al., 2014; Lee, A. K. Y.

20 et al., 2013; Trainic et al., 2011), or acid-base reactions between ammonia/ammonium and organic/inorganic acid species in particles leading to organic ammonium salts (Liu et al., 2012b; Kuwata and Martin, 2012).

Several studies have identified the presence of NOC in laboratory generated SOA associated with the presence of carbonyl groups and NH$_4^+$ (the dominant form of NH$_3$

25 in particles). For example, using an HR-ToF-AMS, N-containing fragments including strong ions at m/z 41, 68, 69 and 70 and weak ions at m/z 46, 52, 53, 57, 68 and 96 have been identified for the uptake of glyoxal on ammonium sulphate particles (Galloway et al., 2009), attributed to imine and/or imidazole formation. Higher molecular

weight N-containing molecular ions such as m/z 97 ($C_4H_5ON_2^+$), 115 ($C_4H_7O_2N_2^+$), 129 ($C_5H_9O_2N_2^+$), 159 ($C_6H_{11}O_3N_2^+$), 173 ($C_7H_{13}O_3N_2^+$), 184 ($C_7H_{10}O_3N_3^+$) have also been detected using high resolution electrospray ionization mass spectrometry (ESI-MS) for the same reaction system (Galloway et al., 2009). In addition, SOA, which was formed through the ozonolysis of d-limonene, subsequently impacted on a polymeric plate and then exposed to gaseous NH$_3$, resulted in a series of amines and imines with one or two N atoms and with molecular weights ranging from 152 to 471 amu, detected by high resolution DESI-MS (Laskin et al., 2010).

Presently, the gas-phase oxidation mechanism of α-pinene by ozone has been fairly well elucidated. In general, the initial step proceeds through cycloaddition of O$_3$ to the C=C bond, forming an excited primary ozonide (POZ). The POZ undergoes a unimolecular isomerization to produce Criegee intermediates (CIs), which subsequently yield both gas-phase and particle-phase compounds containing hydroxyl, carbonyl and acidic functional groups (Zhang and Zhang, 2005; Yu et al., 1999). The OH initialed oxidation mechanism of m-xylene is more complex as described by the Master Chemical Mechanism MCM3.1 (Bloss et al., 2005); however it also leads to particle-phase acids and carbonyls (Loza et al., 2012).

Particle-phase carbonyl compounds are present in the current experiments as confirmed by IR absorption band at 1725 cm^{-1} (in both systems). The observed HR-ToF-AMS fragments families of $C_xH_yN_n$, $C_xH_yON_n$ and $C_xH_yO_2N_n$ indicates that C–N bonds have formed and they are qualitatively similar to those associated with imine and/or imidazole formation (Nguyen et al., 2013; Lee, A. K. Y. et al., 2013) which is generally summarized in Scheme S1. The HR-ToF-AMS fragments and the formation of imine bonds are also consistent with the IR derived functional groups of NH$_x$ and C=N observed in this study (Fig. 2; Table S1).

The formation of organic ammonium salts also cannot be entirely discounted. The NH$_x$ bands in the IR (3490 and 3240 cm^{-1}) as well as the NH$_x$ fragments of the HR-ToF-AMS may arise from the ammonium ion associated with an organic ammonium salt. Although organic acids, whose IR absorbance bands appear at 3300–2500 cm^{-1}

for v_s (OH), 1760–1690 cm^{-1} for v_s (C=O), 1320–1210 cm^{-1} for v_s (C–O), 1440–1395 and 950–910 cm^{-1} for δ(OH) (Lin-Vien et al., 1991) were observed, it is likely that the majority of NH$_x$ arose from the association with acidic sulfate which may need to be fully neutralized prior to the formation of organic salts. Regardless, organic salts would not result in AMS fragments containing N, C and O (i.e.: C$_x$H$_y$N$_n$, C$_x$H$_y$ON$_n$, C$_x$H$_y$O$_2$N$_n$ and NO$_x$) which account for the majority of NOC fragments observed. Finally, the formation of organic ammonium salts is inconsistent with the observed acidity effect on the uptake coefficients leading to NOC (See Sect. 3.6). The mechanisms described above intrinsically assume that heterogeneous reactions occur after the NH$_3$ uptake onto the SOA. However, gas-phase reactions between NH$_3$ and gaseous organic carbonyls and/or acids and subsequent condensation may in principle contribute to the observed particle-phase NOC. However, reactions of NH$_3$/NH$_4^+$ with carbonyls are generally acid catalyzed, as shown in Scheme S1, for both the Schiff base and Mannich reactions. This suggests that if the NOC were gas phase reaction products, a termolecular reaction would be necessary among carbonyls, acid and NH$_3$ in the gas phase; the rates of which are exceedingly slow. Furthermore, gas-phase reactions leading to particle phase NOC should be negligible since the calculated reactive uptake coefficients (γ) of NH$_3$ are positively correlated with particle-phase acidity, and anti-correlated with NH$_3$ concentration as will be discussed in Sect. 3.6. An anti-correlation with the gaseous reactant is characteristic of heterogeneous reactions (Ma et al., 2010).

3.3 Contribution of inorganic and organic NO$_y$ species to NOC

In addition to C$_x$H$_y$N$_n$, C$_x$H$_y$ON$_n$ and C$_x$H$_y$O$_2$N$_n$ fragments as shown in Figs. 1 and S3, strong signals from NO$_x$ (NO$^+$; m/z 30 and NO$_2^+$; m/z 46) are also observed in the particle mass spectra of both VOC systems. These NO$_x$ fragments may have arisen from processes other than the uptake of NH$_3$. NO$_x$ fragments in the HR-ToF-AMS spectra can originate from particle bound NOC, inorganic NO$_y$ (HNO$_3$ or NH$_4$NO$_3$) and/or organic nitrates possibly formed via the chain termination of RO$_2$ or RO radicals

by the trace levels of NO or NO_2 in the chamber. Although zero air was used in this study, trace levels of NO_y (oxides of nitrogen except N_2O) were detected in the chamber as shown in Fig. S4. The maximum NO_y concentration was approximately 0.25 ppbv, but generally much lower.

Figure S5 compares the concentrations of particle-phase NO_x ($NO^+ + NO_2^+$) and total NOC ($T_{NOC} = C_xH_yN_n + C_xH_yON_n + C_xH_yO_2N_n + NO_x$) in a typical SOA experiment with a control experiment performed in the absence of α-pinene (0 ppbv). The NO_x and T_{NOC} concentrations in the control experiment increased only slightly (from 5.4×10^{-17} to 8.4×10^{-17} g particle^{-1} for T_{NOC}) compared to the increases observed in the presence of VOC (from 7.6×10^{-17} to 2.9×10^{-16} g particle^{-1} for T_{NOC}). Assuming that the increase in T_{NOC} in the control experiment was entirely from NO_y, it would contribute a maximum of 14 % of the T_{NOC} mass measured in the typical SOA experiment shown in Fig. S5. In the control experiment NO_x fragments accounted for 74.7 ± 4.9 % of T_{NOC}, hence the possible contribution of inorganic NO_y to T_{NOC} mass in a typical SOA experiment is likely even lower (10.5 ± 0.7) %. This estimation is considered an upper limit to the contributions from inorganic NO_y species, since 0.4 µg m^{-3} of SOA were formed in the control experiment after 6 h of reaction (possibly from the background air of the chamber), suggesting that a small amount of NOC in control experiments may also be formed via the uptake of NH_3 by trace amounts of SOA, which could have contributed at least partially to the NO^+ and NO_2^+ ions in the particle mass spectrum in the control experiment. It should also be pointed out that the OH concentration in a typical oxidation experiment here is likely higher than that in the control experiment, potentially resulting in a higher level of inorganic NO_y.

A further constraint on the contributions of inorganic NO_y to the HR-ToF-AMS fragments at m/z 30 and m/z 46 may be obtained by assuming that all of the measured gaseous NO_y is HNO_3 (in a typical SOA experiment). Under this condition, the solvation of HNO_3 into surface water would contribute to less than 4×10^{-21} g particle^{-1} of HNO_3, calculated using the reported growth factor (GF) of SOA from ozonolysis of α-pinene (1.015 at 50 % RH for 180 nm particle) (Varutbangkul et al., 2006) and the

Title Page

Abstract | Introduction

Conclusions | References

Tables | Figures

|◄ | ►|

◄ | ►

Back | Close

Full Screen / Esc

Printer-friendly Version

Interactive Discussion

Henry's law constant of HNO_3 of $2.1\,mol\,kg^{-1}\,Pa^{-1}$ at 298 K (Lelieveld and Crutzen, 1991). This value is significantly lower than the detected particle NO_x fragment mass concentration in the current experiments ($\sim 10^{-17}\,g\,particle^{-1}$) and suggests that the impact of HNO_3 from the trace level NO_x in the gas phase during the experiments on

5   the particle NOC is negligible. In addition, if both NH_3 and NO_x (ultimately HNO_3) are present in the reaction system, then NH_4NO_3 may be formed (and possibly dissociated into NH_4^+ and NO_3^-). Aqueous NH_4NO_3 (i.e.: NH_4^+ and NO_3^-) can likely be excluded because the RH (50 %) in this study is lower than the deliquescence RH (DRH, 62 %) of NH_4NO_3 (Lightstone et al., 2000). Regardless, the characteristic IR bands of NO_3^-

10 at 1047, 830, and $713\,cm^{-1}$ (Wu et al., 2007), and the strong characteristic IR bands of $NH_4NO_3(s)$ at 1340, 1390 and $1630\,cm^{-1}$ (Miller and Wilkins, 1952) were not observed in Fig. 2. These results imply that a possible interference by inorganic NH_4NO_3 at m/z 30 and 46 is not likely.

While inorganic NO_y (HNO_3 and NH_4NO_3) had little influence on the observed par-

15 ticle NO^+/NO_2^+ fragments (as described above), organic NO_y partitioning may also be possible, leading to NOC that was not derived via the uptake of NH_3. In the presence of NO larger than 10–30 pptv, organonitrates ($RONO_2$) can be formed through reactions between organic peroxy radicals (RO_2) and NO (Arey et al., 2001) and the initial NO concentration in these chamber experiments was ~ 25 pptv (Fig. S6). The

20 limited resolution of the FTIR measurements makes it difficult to differentiate between $RONO_2$ and other NOC bands (~ 1640, 1315, $870\,cm^{-1}$; Fig. 2 and Table S1). However, a number of observations described below suggest that photo-chemically derived $RONO_2$ (hence not NOC from NH_3) was a minor contributor to the observed NO_x fragments, and a further negligible source of $C_xH_yON_n$ and $C_xH_yO_2N_n$ fragments. Firstly,

25 the photo-chemical formation of organo-nitrates in various VOC systems is usually associated with the formation of significantly more HNO_3 (NH_4NO_3 in this study) which was not observed in the IR measurements here. Secondly, AMS measurements have demonstrated that the NO^+/NO_2^+ ratio specifically for monoterpene derived organo-nitrates is in the range of 10–15 (Bruns et al., 2010; Fry et al., 2009), in contrast to

Reactive uptake of ammonia to secondary organic aerosols

Y. Liu et al.

that of the current study (~ 2). Thirdly, Farmer et al. (2010) have shown that $C_xH_yON_n$ and $C_xH_yO_2N_n$ fragments from organo-nitrate standards typically account for < 5 % of the total N containing mass, in contrast to the current study where they account for ~ 30 % (Table 2). Finally, there was an observed positive correlation between particle-phase acidity and the derived uptake coefficients (described in Sect. 3.6) based upon these NOC fragments, which is inconsistent with $RONO_2$ formed photo-chemically in the gas-phase. Consequently, NO_x, $C_xH_yON_n$ and $C_xH_yO_2N_n$ fragments are likely to have arisen primarily from the heterogeneous reactions of NH_3, and are thus included in subsequent kinetic calculations.

3.4 Contribution of NOC to SOA

The temporal evolution of the four families of N-containing fragments (excluding NH_x) and the total SOA during ozonolysis of α-pinene and OH oxidation of m-xylene is shown in Fig. 3a and b respectively. The relative contribution of T_{NOC} to SOA is shown in Fig. 3c and d and summarized for all experiments in Table 2. As shown in Fig. 3a and b, once the ozonolysis or OH oxidation is initiated all N-containing fragments increase significantly with time; but their growth rates were much smaller than that for the bulk of the SOA, as demonstrated by the relatively sharp decline in the T_{NOC}/SOA of Fig. 3c and d. Nonetheless, after 6 h of exposure in these experiments, N-containing species (based upon the quantified HR-ToF-AMS fragments excluding NH_x) contributed 8.9 ± 1.7 and 31.5 ± 4.4 wt% (avg over all experiments) of the total SOA mass from the ozonolysis of α-pinene and OH oxidation of m-xylene, respectively. This is in contrast to recent reports that OH initiated anthropogenic SOA forms relatively less NOC than ozone oxidation of monoterpenes (Updyke et al., 2012). However this is likely dependent upon differences in a variety of conditions between experiments. After 6 h of reaction, as summarized in Table 2, the mean N/C ratio is 0.016 ± 0.004 for the ozonolysis of α-pinene and 0.065 ± 0.011 for the OH oxidation of m-xylene. These N/C ratios are comparable with that of low-volatility oxidized organic aerosol (OOA, 0.011) and a recently isolated nitrogen-enriched OA (0.053) (Su, 2011). In a study of the ozonolysis of d-

Title Page

Abstract | Introduction

Conclusions | References

Tables | Figures

◄ | ►

◄ | ►

Back | Close

Full Screen / Esc

Printer-friendly Version

Interactive Discussion

limonene by Laskin et al. (2010), it was found that < 6 % of the extracted species from fresh SOA contained an N atom, which was ascribed to reactions with trace amounts of NH_3 in the laboratory air or from reactions of dissolved analyte molecules with solvent (acetonitrile). This value (6 %) is comparable with the T_{NOC} content of SOA from the ozonolysis of α–pinene in this study (Table 1). In the reactions between glyoxal and ammonium, N-containing fragments contributed approximately 1 % to the total SOA mass (Chhabra et al., 2010). The diversity in NOC mass fraction or N/C reported previously suggests that the N-containing content of SOA will depend upon the conditions associated with the reaction system, such as the VOC, the oxidant, NH_3 concentration, mass loading of SOA and the seed particle composition. Regardless, the relatively large contribution of T_{NOC} to the formed SOA here suggests that exposure of SOA in the atmosphere to ammonia may be an important mechanism leading to ambient particle phase nitrogen even in the absence of acidic particles (i.e.: exp P5 here). Note that the above fractional NOC values are probably underestimates, as a fraction of the measured NH_x will also arise from NOC, but is not included in the T_{NOC} since the contribution of inorganic ammonium cannot be differentiated.

3.5 Contribution of NOC to Total nitrogen containing mass

The relative contribution of each NOC fragment family to the T_{NOC} is also shown in Fig. 3c and d. The above fragment contribution to T_{NOC}, together with the ratio of T_{NOC} to the total nitrogen containing mass (TN = T_{NOC} + NH_x) and the T_{NOC}/TN ratio on a nitrogen atom mass basis (N_{NOC}/N_{TN}) are summarized for all experiments in Table 2. After 6 h of NH_3 exposure (Fig. 3c), the ratio of NO_x, $C_xH_yN_n$, $C_xH_yON_n$ and $C_xH_yO_2N_n$ fragment families to T_{NOC} were 37.2, 33.5, 17.0 and 12.2 wt%, respectively for the ozonolysis of α–pinene, and 45.6, 34.3, 15.7 and 4.5 wt% for the OH oxidation of m-xylene (Fig. 3d). These relative contributions to T_{NOC} were consistent between experiments and VOC systems, with the exception of $C_xH_yO_2N_n$ fragments which contributed approximately 3 times less to the T_{NOC} in m-xylene experiments compared to those of α-pinene (Table 2). Placed in the context of the total nitrogen containing mass (TN),

which includes the inorganic ammonium, NOC formed from exposure of SOA to NH_3 accounted for a substantial fraction of the TN ($\sim$ 10–20 wt%) with a generally greater contribution in the m-xylene system under otherwise similar conditions. However, a better indication of the importance of NOC forming reactions is derived by computing the above ratio on an atomic nitrogen mass basis (N_{NOC}/N_{TN}; Table 2). Despite the carbon, hydrogen and oxygen content of the NOC fragments, the amount of N associated with NOC remains a significant contributor to the total N mass ($\sim$ 4–15 wt%), and is likely underestimated since an unknown fraction of NH_x will be from NOC. Such a high N content in these particles may have implications for ambient particulate nitrogen loading and subsequent N deposition which will be discussed further in Sect. 4.

3.6 Reaction kinetics

Typical temporal profiles for T_{NOC} during the ozonolysis of α-pinene, which are used in the kinetic calculations, can be represented by those for Exp. P3 and P5 (Fig. 4). The open circles and solid triangles represent the experimental data, with the fit of the uptake model shown as red and blue lines during the initial (from 0 to 150 min) and the final stages (from 400 to 1250 min) of the experiment, respectively. In these specific experiments (P3, P5), the observed initial reactive uptake coefficients of NH_3 ($\gamma_{obs, ini}$; on an atomic N mass basis) to form the N in NOC were $4.8 \pm 0.2 \times 10^{-3}$ and $1.07 \pm 0.03 \times 10^{-3}$ respectively. The final uptake coefficients ($\gamma_{t, ini}$) were obtained by performing gas-phase diffusion corrections for NH_3 using a previously reported empirical formula (Fuchs and Sutugin, 1970; Worsnop et al., 2002; Widmann and Davis, 1997) and the diffusion coefficient of NH_3 in air ($0.1978 \, cm^2 \, s^{-1}$) (Massman, 1998). The corresponding $\gamma_{t, ini}$ values for all experiments ranged from $1.23 \pm 0.04 \times 10^{-3}$ to $1.52 \pm 0.03 \times 10^{-2}$ (Table 2). As discussed above, a fraction of the observed NH_x fragments are likely to have arisen from NOC. However they are not included in the uptake coefficient estimates of Table 2 and thus results in an underestimate of γ. Conversely, including NH_x in the calculation of γ (Table S2) is considered an overestimate. Despite

this uncertainty, these uptake coefficients on the order of 10^{-3} are relatively large. At present time, no data is available for comparison since the uptake kinetics of NH_3 on organic aerosol has not been reported. However, the uptake coefficients measured in this study are similar to those observed for glyoxal (Liggio et al., 2005b, a; Liggio and Li, 2006a), and are 2–4 orders of magnitude higher than biogenic olefins (Liggio and Li, 2008) and pinonaldehydie (Liggio and Li, 2006a) on acidic surfaces.

While not included in the derivation of γ leading to NOC, the NH_x data from these experiments can be used to derive NH_3 uptake coefficients leading to inorganic ammonium (γ_{NH_4}) using the same approach as above. The resultant γ_{NH_4} values are given in Table S2 and range from 5.3×10^{-4} to 1.78×10^{-2} (mean = 6.4×10^{-3}) comparable to the range of 4×10^{-3}–2×10^{-4} reported for the competing uptake of NH_3 with ambient organic gases by sulfuric acid (Liggio et al., 2011). The current uptake coefficients leading to NH_4^+ are similar in magnitude to those leading to NOC, and significantly less than what would be expected based upon the neutralization of sulfuric acid particle ($\sim$ 0.5–1; Swartz et al., 1999). These results suggest that under these conditions, the formation of NOC can compete with the neutralization of acidic particle, possibly due to kinetic limitations on the uptake of NH_3 caused by the coating of SOA as has been demonstrated previously (Liggio et al., 2011).

3.7 Factors affecting reaction kinetics

To determine the uptake kinetics of NH_3 by relatively aged SOA during ozonolysis of α–pinene or OH oxidation of m-xylene additional ammonia (Δc: $\sim$ 30 ppbv) was introduced into the reaction chamber after approximately 6 h of the original exposure. As shown in Fig. 3a and b, the additional NH_3 did not result in a change in the absolute concentration of N-containing species in the SOA. The ratio of TN to SOA increased slightly in the last half of the experiments, possibly due to the evaporation of SOA when α–pinene was entirely consumed or further particle-phase oxidation by oxidants (OH and/or O_3). A reduced uptake of NH_3 for the more aged SOA is also reflected in the

derived uptake coefficients from the latter stages of the experiments. After 400 min of reaction (Fig. 4), the NOC uptake had slowed significantly, and the derived uptake coefficients of NH_3 to form NOC decreased to $1.61 \pm 0.24 \times 10^{-5}$ and $4.01 \pm 0.13 \times 10^{-5}$, respectively.

5   A number of factors may explain the reduced uptake onto the more aged particles of these experiments (> 400 min; Fig. 4). Firstly, this may suggest that in the latter stages of photo-chemistry, multi-generational particle-phase products of VOC oxidation contain functional groups not involved in the NOC forming heterogeneous reactions. However, the change in the O/C ratio during these experiments was quite small;
10 increasing from 0.4 to 0.46 over 6 h (Fig. S7). At the same time, precursor VOCs were not fully depleted after 6 h, suggesting that carbonyls should continue to be formed throughout the experiment and not be entirely consumed via a heterogeneous reaction with NH_3. Given that the postulated heterogeneous reactions (Mannich reaction and/or Schiff base reaction) are known to be acid catalyzed (Mitsumori et al., 2006), we sug-
15 gest that a diffusion limitation to the acidic core of the particle (or to a region where acidity and carbonyls are unavailable) may be responsible for the slow decrease in uptake with time as significant organic material (SOA) is added to the seed particles. This would have the effect of reducing the uptake of NH_3 leading to both NOC and NH_4^+, consistent with the derived γ of both. In particular, the formation of oligomers of high
20 molecular weight (which may be more likely to hinder liquid phase diffusion) has been noted to occur in various SOA systems (Kalberer et al., 2004; Gross et al., 2006). This is also consistent with previous laboratory studies in which a high NH_3 exposure for several days is required to detect the BrC in SOA (Nguyen et al., 2013; Lee, H. J. et al., 2013; Updyke et al., 2012). The current results suggest that the formation of NOC from
25 NH_3 uptake will be more efficient for newly formed SOA (which is accelerated in the presence of sulfuric acid) compared to aged SOA.

    The relationship between $\gamma_{t, ini}$ and the particle-phase acidity for the ozonolysis of α-pinene is shown in Fig. 5. Since the RH (50 ± 2 %) was lower than the deliquescence RH (DRH) of the mixtures of H_2SO_4-Na_2SO_4 used (~ 80 %), we cannot reasonably

estimate the surface pH with the E-AIM model (Friese and Ebel, 2010), though it is expected that some surface coverage of water likely exists. Alternatively, the mole ratio of H_2SO_4 to Na_2SO_4 is used as a qualitative metric for the acidity in Fig. 5. Namely, a higher ratio of H_2SO_4/Na_2SO_4 indicates stronger acidity. As shown in Fig. 5, the reactive uptake coefficient for the T_{NOC} ($\gamma_{t,\,ini}$) increased by approximately a factor of 4 with increasing particle-phase acidity. This is consistent with the previously postulated acid-catalyzed reaction mechanisms between carbonyls and NH_3 or NH_4^+ (in equilibrium with gas phase NH_3) in Scheme 1 and elsewhere (Nguyen et al., 2013; Bones et al., 2010). In Fig. 5, an upper and lower limit to this qualitative relationship with acidity is estimated by including and excluding NH_x in the derivation of $\gamma_{t,\,ini}$, both of which bear the same relationship.

Further insight into the controlling factors in this system is also gained from the relationship between $\gamma_{t,\,ini}$ and gaseous NH_3, which is shown in Fig. 6, for a fixed particle-phase acidity (H_2SO_4/Na_2SO_4 in moles: 1.95). These figures demonstrate that $\gamma_{t,\,ini}$ for T_{NOC} decreases with increases in NH_3 (g) concentration (regardless of the inclusion of NH_x into γ). In other reaction systems, an anti-correlation between uptake coefficients and gaseous reactant has been used to indicate that heterogeneous reactions occur on the particle surface, limited by an increasing number of ineffective collisions between the reactive sites and the gaseous reactant (i.e.: surface saturation; Ma et al., 2010; Poschl et al., 2001; Mmereki and Donaldson, 2003; Kwamena et al., 2004). While this possibility cannot be ruled out here, the above acidity dependence argues against surface reaction, since a hydrophilic acidic seed is unlikely to be miscible with a somewhat hydrophobic SOA and thus migrate to the surface. Rather, we hypothesize that the relationship in Fig. 6 is driven by the kinetics of organic $+ NH_3/NH_4^+$ reactions that lead to the NOC. In this scenario, a larger $\gamma_{t,\,ini}$ would be observed at lower NH_3 concentration when NH_3 and/or NH_4^+ in the particle is rate limiting, and a reduced $\gamma_{t,\,ini}$ at higher NH_3 (Fig. 6) observed when the organic reactant is the rate limiting reagent in the formation of NOC. This argument is also consistent with a decrease in the T_{NOC} fraction of SOA with increasing SOA mass added as shown in Fig. 7, and again suggests that a bar-

rier/diffusion limitation caused by organic coatings limits the formation of NOC in these experiments. The relatively few data points of Fig. 7 underlie the need for further systematic study to conclusively determine the controlling factors leading to the formation of NOC.

4   Implications

Organonitrogen compounds have been regarded as an important class of brown carbon in atmospheric particles, and may also have an influence on regional and global N deposition. As shown in this work, NOC compounds can be formed efficiently and quickly via the uptake of NH_3 by newly formed SOA, in contrast to other studies where NOC forms over several days (Bones et al., 2010). If it is assumed that a steady state between NOC and SOA is established as observed in this study (i.e.: Figs. 3 and 4), then a crude estimate of the formation rate of ambient NOC via the uptake of NH_3 to biogenic SOA (BSOA) and anthropogenic SOA (ASOA) can be derived. Top-down estimates of global biogenic BSOA and anthropogenic ASOA formation have been estimated at approximately 88 and $10\,Tg\,C\,yr^{-1}$, respectively (Hallquist et al., 2009; Farina et al., 2010). Based upon the measured ratio of NOC in SOA (i.e. (8.8 ± 1.7) wt% for ozonolysis of α-pinene and (31.5 ± 4.4) wt% for OH oxidation of m-xylene after 6 h) and a value 1.4 for OM/OC (Hallquist et al., 2009) the estimated global NOC via the reactive uptake of NH_3 are then 10.8 ± 2.1 and $4.4 \pm 0.6\,Tg\,yr^{-1}$ from BSOA and ASOA respectively, given sufficient NH_3 availability. However, it should be noted that the lowest NH_3 concentration used in this study was significantly higher than that typically found in troposphere. While the dependence of the NOC/SOA on NH_3 concentration was weak in this high concentration regime, it is not clear if it remains so at more relevant NH_3 levels. In addition, the formation of NOC may not reach a steady state in the atmosphere, as NH_3, SOA and acidic sulfate can be present simultaneously, preventing the formation of an organic barrier as hypothesized in this study. The MAC of both BSOA and ASOA is known to be enhanced by NH_3 aging (Updyke et al., 2012) however only

to a maximum of $\sim 0.1\,\mathrm{m^2\,g^{-1}}$ at 500 nm wavelength. When compared to black carbon, with a MAC of $> 10\,\mathrm{m^2\,g^{-1}}$ (Updyke et al., 2012) and a global emission of $\sim 8\,\mathrm{Tg\,yr^{-1}}$ (Bond et al., 2004), the contribution of NOC originating from the uptake of NH_3 by SOA to light absorption and the overall energy budget is likely to be small. It should be noted

5 that light absorption by NOC may be relatively more important in the UV range, where NOC should have much higher MAC. While this may not change the energy budget as significantly as black carbon, the actinic flux could be significantly changed, with different consequences. However, light absorption by NOC in atmospheric particles may be important regionally where the BC contribution is minimal.

10 Based upon the mean N/C in SOA after 6 h of reaction ($1.6 \pm 0.4 \times 10^{-2}$; α-pinene and $6.5 \pm 1.1 \times 10^{-2}$; m-xylene), the uptake of NH_3 by BSOA and ASOA may contribute up to 1.4 ± 0.4 and $0.7 \pm 0.1\,\mathrm{Tg\,N\,yr^{-1}}$ from the reactive uptake of NH_3. Although these values are significantly less than the total global emission of NH_3 ($33.4\,\mathrm{Tg\,N\,yr^{-1}}$) (Reis et al., 2009), it may be important on a local or regional scale. The similarity between the

15 uptake coefficients for NOC and inorganic NH_4^+ suggests that in the presence of organic coatings, NOC formation can compete with particle neutralization. Furthermore, under the conditions of these experiments up to 15 % of the total N mass is attributed to NOC. If this value holds true for the ambient atmosphere, then a significant portion of N in PM is miss-represented as NH_4^+ or entirely unaccounted for. This will provide a means

20 to transport more N further from ammonia sources and result in N deposition patterns poorly predicted by regional models (Cornell et al., 2003; Cape et al., 2011). Although a more thorough modelling study and further insight into the rates and mechanisms of NOC formation is required to clearly elucidate its impact on climate and regional nitrogen deposition, the result of this study suggest that NOC from NH_3 should be

25 considered with respect to overall deposition of N to sensitive ecosystems.

The Supplement related to this article is available online at doi:10.5194/acpd-15-17449-2015-supplement.

References

Aiken, A. C., Peter, F. DeCarlo, P. F., and Jimenez, J. L.: Elemental analysis of organic species with electron ionization high-resolution mass spectrometry, Anal. Chem., 79, 8350–8358, doi:10.1021/ac071150w, 2007.

Alexander, D. T. L., Crozier, P. A., and Anderson, J. R.: Brown carbon spheres in East Asian outflow and their optical properties, Science, 321, 833–836, doi:10.1126/science.1155296, 2008.

Andrade-Eiroa, A., Leroy, V., Dagaut, P., and Bedjanian, Y.: Determination of polycyclic aromatic hydrocarbons in kerosene and bio-kerosene soot, Chemosphere, 78, 1342–1349, doi:10.1016/j.chemosphere.2010.01.005, 2010.

Andreae, M. O. and Gelencsér, A.: Black carbon or brown carbon? The nature of light-absorbing carbonaceous aerosols, Atmos. Chem. Phys., 6, 3131–3148, doi:10.5194/acp-6-3131-2006, 2006.

Arey, J., Aschmann, S. M., Kwok, E. S. C., and Atkinson, R.: Alkyl nitrate, hydroxyalkyl nitrate, and hydroxycarbonyl formation from the NO_x-air photooxidations of C_5-C_8 n-alkanes, J. Phys. Chem. A., 105, 1020–1027, doi:10.1021/jp003292z, 2001.

Beddows, D. C. S., Donovan, R. J., Harrison, R. M., Heal, M. R., Kinnersley, R. P., King, M. D., Nicholson, D. H., and Thompson, K. C.: Correlations in the chemical composition of rural background atmospheric aerosol in the UK determined in real time using Time-of-Flight Mass Spectrometry, J. Environ. Monitor., 6, 124–133, doi:10.1039/b311209h, 2004.

Bloss, C., Wagner, V., Jenkin, M. E., Volkamer, R., Bloss, W. J., Lee, J. D., Heard, D. E., Wirtz, K., Martin-Reviejo, M., Rea, G., Wenger, J. C., and Pilling, M. J.: Development of a detailed chemical mechanism (MCMv3.1) for the atmospheric oxidation of aromatic hydrocarbons, Atmos. Chem. Phys., 5, 641–664, doi:10.5194/acp-5-641-2005, 2005.

Bond, T. C., Streets, D. G., Yarber, K. F., Nelson, S. M., Woo, J.-H., and Klimont, Z.: A technology-based global inventory of black and organic carbon emissions from combustion, J. Geophys. Res.-Atmos., 109, D14203, doi:10.1029/2003JD003697, 2004.

Reactive uptake of ammonia to secondary organic aerosols

Y. Liu et al.

Title Page

Abstract	Introduction
Conclusions	References
Tables	Figures

|◀ | ▶|

◀ | ▶

Back | Close

Full Screen / Esc

Printer-friendly Version

Interactive Discussion

Bond, T. C., Doherty, S. J., Fahey, D. W., Forster, P. M., Berntsen, T., DeAngelo, B. J., Flanner, M. G., Ghan, S., Kärcher, B., Koch, D., Kinne, S., Kondo, Y., Quinn, P. K., Sarofim, M. C., Schultz, M. G., Schulz, M., Venkataraman, C., Zhang, H., Zhang, S., Bellouin, N., Guttikunda, S. K., Hopke, P. K., Jacobson, M. Z., Kaiser, J. W., Klimont, Z., Lohmann, U., Schwarz, J. P., Shindell, D., Storelvmo, T., Warren, S. G., and Zender, C. S.: Bounding the role of black carbon in the climate system: a scientific assessment, J. Geophys. Res.-Atmos., 118, 5380–5552, doi:10.1002/jgrd.50171, 2013.

Bones, D. L., Henricksen, D. K., Mang, S. A., Gonsior, M., Bateman, A. P., Nguyen, T. B., Cooper, W. J., and Nizkorodov, S. A.: Appearance of strong absorbers and fluorophores in limonene-O(3) secondary organic aerosol due to NH(4) (+)-mediated chemical aging over long time scales, J. Geophys. Res.-Atmos., 115, D05203, doi:10.1029/2009JD012864, 2010.

Bruns, E. A., Perraud, V., Zelenyuk, A., Ezell, M. J., Johnson, S. N., Yu, Y., Imre, D., Finlayson-Pitts, B. J., and Alexander, M. L.: Comparison of FTIR and particle mass spectrometry for the measurement of particulate organic nitrates, Environ. Sci. Technol., 44, 1056–1061, doi:10.1021/es9029864, 2010.

Bunce, N. J., Liu, L., Zhu, J., and Lane, D. A.: Reaction of naphthalene and its derivatives with hydroxyl radicals in the gas phase, Environ. Sci. Technol., 31, 2252–2259, doi:10.1021/es960813g, 1997.

Bzdek, B. R., Ridge, D. P., and Johnston, M. V.: Amine exchange into ammonium bisulfate and ammonium nitrate nuclei, Atmos. Chem. Phys., 10, 3495–3503, doi:10.5194/acp-10-3495-2010, 2010.

Cape, J. N., Cornell, S. E., Jickells, T. D., and Nemitz, E.: Organic nitrogen in the atmosphere – where does it come from? A review of sources and methods, Atmos. Res., 102, 30–48, doi:10.1016/j.atmosres.2011.07.009, 2011.

Cappa, C. D., Onasch, T. B., Massoli, P., Worsnop, D. R., Bates, T. S., Cross, E. S., Davidovits, P., Hakala, J., Hayden, K. L., Jobson, B. T., Kolesar, K. R., Lack, D. A., Lerner, B. M., Li, S.-M., Mellon, D., Nuaaman, I., Olfert, J. S., Petäjä, T., Quinn, P. K., Song, C., Subramanian, R., Williams, E. J., and Zaveri, R. A.: Radiative absorption enhancements due to the mixing state of atmospheric black carbon, Science, 337, 1078–1081, doi:10.1126/science.1223447, 2012.

Reactive uptake of ammonia to secondary organic aerosols

Y. Liu et al.

Title Page

Abstract	Introduction
Conclusions	References
Tables	Figures

|◄ | ►|

◄ | ►

Back | Close

Full Screen / Esc

Printer-friendly Version

Interactive Discussion

Chan, L. P. and Chan, C. K.: Displacement of ammonium from aerosol particles by uptake of triethylamine, Aerosol Sci. Technol., 46, 236–247, doi:10.1080/02786826.2011.618815, 2012.

Cheng, Y., Li, S.-M., and Leithead, A.: Chemical characteristics and origins of nitrogen-containing organic compounds in $PM_{2.5}$ aerosols in the Lower Fraser Valley, Environ. Sci. Technol., 40, 5846–5852, doi:10.1021/es0603857, 2006

Chhabra, P. S., Flagan, R. C., and Seinfeld, J. H.: Elemental analysis of chamber organic aerosol using an aerodyne high-resolution aerosol mass spectrometer, Atmos. Chem. Phys., 10, 4111–4131, doi:10.5194/acp-10-4111-2010, 2010.

Cornell, S. E., Jickells, T. D., Cape, J. N., Rowland, A. P., and Duce, R. A.: Organic nitrogen deposition on land and coastal environments: a review of methods and data, Atmos. Environ., 37, 2173–2191, doi:10.1016/S1352-2310(03)00133-X, 2003.

Darer, A. I., Cole-Filipiak, N. C., O'Connor, A. E., and Elrod, M. J.: Formation and stability of atmospherically relevant isoprene-derived organosulfates and organonitrates, Environ. Sci. Technol., 45, 1895–1902, doi:10.1021/es103797z, 2011.

DeCarlo, P. F., Kimmel, J. R., Trimborn, A., Northway, M. J., Jayne, J. T., Aiken, A. C., Gonin, M., Fuhrer, K., Horvath, T., Docherty, K. S., Worsnop, D. R., and Jimenez, J. L.: Field-deployable, high-resolution, Time-of-Flight Aerosol Mass Spectrometer, Anal. Chem., 78, 8281–8289, doi:10.1021/ac061249n, 2006.

Donahue, N. M., Henry, K. M., Mentel, T. F., Kiendler-Scharr, A., Spindler, C., Bohn, B., Brauers, T., Dorn, H. P., Fuchs, H., Tillmann, R., Wahner, A., Saathoff, H., Naumann, K.-H., Möhler, O., Leisner, T., Müller, L., Reinnig, M.-C., Hoffmann, T., Salo, K., Hallquist, M., Frosch, M., Bilde, M., Tritscher, T., Barmet, P., Praplan, A. P., DeCarlo, P. F., Dommen, J., Prévôt, A. S. H., and Baltensperger, U.: Aging of biogenic secondary organic aerosol via gas-phase OH radical reactions, P. Natl. Acad. Sci. USA, 109, 13503–13508, doi:10.1073/pnas.1115186109, 2012.

Farina, S. C., Adams, P. J., and Pandis, S. N.: Modeling global secondary organic aerosol formation and processing with the volatility basis set: implications for anthropogenic secondary organic aerosol, J. Geophys. Res.-Atmos., 115, D09202, doi:10.1029/2009JD013046, 2010.

Farmer, D. K., Matsunaga, A., Docherty, K. S., Surratt, J. D., Seinfeld, J. H., Ziemann, P. J., and Jimenez, J. L.: Response of an aerosol mass spectrometer to organonitrates and organosulfates and implications for atmospheric chemistry, P. Natl. Acad. Sci. USA, 107, 6670–6675, doi:10.1073/pnas.0912340107, 2010.

Friese, E. and Ebel, A.: Temperature dependent thermodynamic model of the system H^+–NH_4^+–Na^+–SO_4^{2-}–NO_3^-–Cl^-–H_2O, J. Phys. Chem. A., 114, 11595–11631, doi:10.1021/jp101041j, 2010.

Fry, J. L., Kiendler-Scharr, A., Rollins, A. W., Wooldridge, P. J., Brown, S. S., Fuchs, H., Dubé, W., Mensah, A., dal Maso, M., Tillmann, R., Dorn, H.-P., Brauers, T., and Cohen, R. C.: Organic nitrate and secondary organic aerosol yield from NO_3 oxidation of β-pinene evaluated using a gas-phase kinetics/aerosol partitioning model, Atmos. Chem. Phys., 9, 1431–1449, doi:10.5194/acp-9-1431-2009, 2009.

Fuchs, N. A. and Sutugin, A. G.: Highly Dispersed Aerosols, Butterworth-Heinemann, Newton, MA, 1970.

Galloway, M. M., Chhabra, P. S., Chan, A. W. H., Surratt, J. D., Flagan, R. C., Seinfeld, J. H., and Keutsch, F. N.: Glyoxal uptake on ammonium sulphate seed aerosol: reaction products and reversibility of uptake under dark and irradiated conditions, Atmos. Chem. Phys., 9, 3331–3345, doi:10.5194/acp-9-3331-2009, 2009.

García-Gómez, H., Garrido, J. L., Vivanco, M. G., Lassaletta, L., Rábago, I., Àvila, A., Tsyro, S., Sánchez, G., González Ortiz, A., González-Fernández, I., and Alonso, R.: Nitrogen deposition in Spain: modeled patterns and threatened habitats within the Natura 2000 network, Sci. Total Environ., 485–486, 450–460, doi:10.1016/j.scitotenv.2014.03.112, 2014.

Gross, D. S., Gälli, M. E., Kalberer, M., Prevot, A. S. H., Dommen, J., Alfarra, M. R., Duplissy, J., Gaeggeler, K., Gascho, A., Metzger, A., and Baltensperger, U.: Real-time measurement of oligomeric species in secondary organic aerosol with the aerosol Time-of-Flight Mass Spectrometer, Anal. Chem., 78, 2130–2137, doi:10.1021/ac060138l, 2006.

Hallquist, M., Wenger, J. C., Baltensperger, U., Rudich, Y., Simpson, D., Claeys, M., Dommen, J., Donahue, N. M., George, C., Goldstein, A. H., Hamilton, J. F., Herrmann, H., Hoffmann, T., Iinuma, Y., Jang, M., Jenkin, M. E., Jimenez, J. L., Kiendler-Scharr, A., Maenhaut, W., McFiggans, G., Mentel, Th. F., Monod, A., Prévôt, A. S. H., Seinfeld, J. H., Surratt, J. D., Szmigielski, R., and Wildt, J.: The formation, properties and impact of secondary organic aerosol: current and emerging issues, Atmos. Chem. Phys., 9, 5155–5236, doi:10.5194/acp-9-5155-2009, 2009.

Hawkins, L. N., Russell, L. M., Covert, D. S., Quinn, P. K., and Bates, T. S.: Carboxylic acids, sulfates, and organosulfates in processed continental organic aerosol over the southeast Pacific Ocean during VOCALS-REx 2008, J. Geophys. Res.-Atmos., 115, D13201, doi:10.1029/2009jd013276, 2010.

Title Page

Abstract | Introduction

Conclusions | References

Tables | Figures

|◀ | ▶|

◀ | ▶

Back | Close

Full Screen / Esc

Printer-friendly Version

Interactive Discussion

Heald, C. L., Collett Jr., J. L., Lee, T., Benedict, K. B., Schwandner, F. M., Li, Y., Clarisse, L., Hurtmans, D. R., Van Damme, M., Clerbaux, C., Coheur, P.-F., Philip, S., Martin, R. V., and Pye, H. O. T.: Atmospheric ammonia and particulate inorganic nitrogen over the United States, Atmos. Chem. Phys., 12, 10295–10312, doi:10.5194/acp-12-10295-2012, 2012.

Iinuma, Y., Böge, O., Kahnt, A., and Herrmann, H.: Laboratory chamber studies on the formation of organosulfates from reactive uptake of monoterpene oxides, Phys. Chem. Chem. Phys., 11, 7985–7997, doi:10.1039/b904025k, 2009.

Kalberer, M., Paulsen, D., Sax, M., Steinbacher, M., Dommen, J., Prevot, A. S. H., Fisseha, R., Weingartner, E., Frankevich, V., Zenobi, R., and Baltensperger, U.: Identification of polymers as major components of atmospheric organic aerosols, Science, 303, 1659–1662, doi:10.1126/science.1092185, 2004.

Kinsey, J. S., Hays, M. D., Dong, Y., Williams, D. C., and Logan, R.: Chemical characterization of the fine particle emissions from commercial aircraft engines during the Aircraft Particle Emissions eXperiment (APEX) 1 to 3, Environ. Sci. Technol., 45, 3415–3421, doi:10.2514/1.36371, 2011.

Kosterev, A. A., Curl, R. F., Tittel, F. K., Kohler, R., Gmachl, C., Capasso, F., Sivco, D. L., and Cho, A. Y.: Transportable automated ammonia sensor based on a pulsed thermoelectrically cooled quantum-cascade distributed feedback laser, Appl. Optics, 41, 573–578, doi:10.1364/ao.41.000573, 2002.

Kourtchev, I., O'Connor, I. P., Giorio, C., Fuller, S. J., Kristensen, K., Maenhaut, W., Wenger, J. C., Sodeau, J. R., Glasius, M., and Kalberer, M.: Effects of anthropogenic emissions on the molecular composition of urban organic aerosols: an ultrahigh resolution mass spectrometry study, Atmos. Environ., 89, 525–532, doi:10.1016/j.atmosenv.2014.02.051, 2014.

Kuwata, M. and Martin, S. T.: Phase of atmospheric secondary organic material affects its reactivity, P. Natl. Acad. Sci. USA, 109, 17354–17359, doi:10.1073/pnas.1209071109, 2012.

Kwamena, N.-O. A., Thornton, J. A., and Abbatt, J. P. D.: Kinetics of surface-bound benzo[a]pyrene and ozone on solid organic and salt aerosols, J. Phys. Chem. A., 108, 11626–11634, doi:10.1021/jp046161x, 2004.

Laskin, J., Laskin, A., Roach, P. J., Slysz, G. W., Anderson, G. A., Nizkorodov, S. A., Bones, D. L., and Nguyen, L. Q.: High-resolution desorption electrospray ionization mass spectrometry for chemical characterization of organic aerosols, Anal. Chem., 82, 2048–2058, doi:10.1021/ac902801f, 2010.

Reactive uptake of ammonia to secondary organic aerosols

Y. Liu et al.

Title Page

Abstract | Introduction

Conclusions | References

Tables | Figures

|◄ | ►|

◄ | ►

Back | Close

Full Screen / Esc

Printer-friendly Version

Interactive Discussion

Lee, A. K. Y., Zhao, R., Li, R., Liggio, J., Li, S.-M., and Abbatt, J. P. D.: Formation of light absorbing organo-nitrogen species from evaporation of droplets containing glyoxal and ammonium sulfate, Environ. Sci. Technol., 47, 12819–12826, doi:10.1021/es402687w, 2013.

Lee, H. J., Laskin, A., Laskin, J., and Nizkorodov, S. A.: Excitation emission spectra and fluorescence quantum yields for fresh and aged biogenic secondary organic aerosols, Environ. Sci. Technol., 47, 5763–5770, doi:10.1021/es400644c, 2013.

Lelieveld, J. and Crutzen, P. J.: The role of clouds in tropospheric photochemistry, J. Atmos. Chem., 12, 229–267, doi:10.1007/BF00048075, 1991.

Liggio, J. and Li, S. M.: Reactive uptake of pinonaldehyde on acidic aerosols, J. Geophys. Res.-Atmos., 111, D24303, doi:10.1029/2005JD006978, 2006a.

Liggio, J. and Li, S. M.: Organosulfate formation during the uptake of pinonaldehyde on acidic sulfate aerosols, Geophys. Res. Lett., 33, L13808, doi:10.1029/2006GL026079, 2006b.

Liggio, J. and Li, S.-M.: Reversible and irreversible processing of biogenic olefins on acidic aerosols, Atmos. Chem. Phys., 8, 2039–2055, doi:10.5194/acp-8-2039-2008, 2008.

Liggio, J., Li, S. M., and McLaren, R.: Heterogeneous reactions of glyoxal on particulate matter: identification of acetals and sulfate esters, Environ. Sci. Technol., 39, 1532–1541, doi:10.1021/es048375y, 2005a.

Liggio, J., Li, S. M., and McLaren, R.: Reactive uptake of glyoxal by particulate matter, J. Geophys. Res.-Atmos., 110, D10304, doi:10.1029/2004jd005113, 2005b.

Liggio, J., Li, S.-M., Vlasenko, A., Stroud, C., and Makar, P.: Depression of ammonia uptake to sulfuric acid aerosols by competing uptake of ambient organic gases, Environ. Sci. Technol., 45, 2790–2796, doi:10.1021/es103801g, 2011.

Lightstone, J. M., Onasch, T. B., Imre, D., and Oatis, S.: Deliquescence, efflorescence, and water activity in ammonium nitrate and mixed ammonium nitrate/succinic acid microparticles, J. Phys. Chem. A., 104, 9337–9346, doi:10.1021/jp002137h, 2000.

Lin-Vien, D., Colthup, N. B., Fateley, W. G., and Grasselli, J. G.: The Handbook of Infrared and Raman Characteristic Frequencies of Organic Molecules, Academic Press Limited, London NWI7DX, UK, 1991.

Liu, X., Zhang, Y., Han, W., Tang, A., Shen, J., Cui, Z., Vitousek, P., Erisman, J. W., Goulding, K., Christie, P., Fangmeier, A., and Zhang, F.: Enhanced nitrogen deposition over China, Nature, 494, 459–462, 2013.

Title Page

Abstract | Introduction

Conclusions | References

Tables | Figures

|◀ | ▶|

◀ | ▶

Back | Close

Full Screen / Esc

Printer-friendly Version

Interactive Discussion

Liu, Y., Han, C., Liu, C., Ma, J., Ma, Q., and He, H.: Differences in the reactivity of ammonium salts with methylamine, Atmos. Chem. Phys., 12, 4855–4865, doi:10.5194/acp-12-4855-2012, 2012a.

Liu, Y., Ma, Q., and He, H.: Heterogeneous uptake of amines by citric acid and humid acid, Environ. Sci Technol., 46, 11112–11118, doi:10.1021/es302414v, 2012b.

Loza, C. L., Chhabra, P. S., Yee, L. D., Craven, J. S., Flagan, R. C., and Seinfeld, J. H.: Chemical aging of *m*-xylene secondary organic aerosol: laboratory chamber study, Atmos. Chem. Phys., 12, 151–167, doi:10.5194/acp-12-151-2012, 2012.

Ma, J., Liu, Y., and He, H.: Degradation kinetics of anthracene by ozone on mineral oxides, Atmos. Environ., 44, 4446–4453, doi:10.1016/j.atmosenv.2010.07.042, 2010

Massman, W. J.: A review of the molecular diffusivtives of H_2O, CO_2, CH_4, CO, O_3, SO_2, NH_3, N_2O, NO, and NO_2 in air, O_2 and N_2 near STP, Atmos. Environ., 32, 1111–1127, doi:10.1016/S1352-2310(97)00391-9, 1998.

Miller, F. A. and Wilkins, C. H.: Infrared spectra and characteristic frequencies of inorganic ions, Anal. Chem., 24, 1253–1294, doi:10.1021/ac60068a007, 1952.

Mitsumori, S., Zhang, H., Cheong, P. H. Y., Houk, K. N., Tanaka, F., and Barbas, C. F.: Direct asymmetric *anti*-Mannich-type reactions catalyzed by a designed amino acid, J. Am. Chem. Soc., 128, 1040–1041, doi:10.1021/ja056984f, 2006.

Mmereki, B. T. and Donaldson, D. J.: Direct observation of the kinetics of an atmospherically important reaction at the air-aqueous interface, J. Phys. Chem. A, 107, 11038–11042, doi:10.1021/jp036119m, 2003.

Nguyen, Q. T., Kristensen, T. B., Hansen, A. M. K., Skov, H., Bossi, R., Massling, A., Sorensen, L. L., Bilde, M., Glasius, M., and Nojgaard, J. K.: Characterization of humic-like substances in Arctic aerosols, J. Geophys. Res.-Atmos., 119, 5011–5027, doi:10.1002/2013jd020144, 2014.

Nguyen, T. B., Lee, P. B., Updyke, K. M., Bones, D. L., Laskin, J., Laskin, A., and Nizkorodov, S. A.: Formation of nitrogen- and sulfur-containing light-absorbing compounds accelerated by evaporation of water from secondary organic aerosols, J. Geophys. Res.-Atmos., 117, D01207, doi:10.1029/2011JD016944, 2012.

Nguyen, T. B., Laskin, A., Laskin, J., and Nizkorodov, S. A.: Brown carbon formation from ketoaldehydes of biogenic monoterpenes, Faraday Discuss., 165, 473–494, doi:10.1039/C3FD00036B, 2013.

Title Page

Abstract | Introduction

Conclusions | References

Tables | Figures

◀ | ▶|

◀ | ▶

Back | Close

Full Screen / Esc

Printer-friendly Version

Interactive Discussion

Pöschl, U., Letzel, T., Schauer, C., and Niessner, R.: Interaction of ozone and water vapor with spark discharge soot aerosol particles coated with benzo[a]pyrene: O_3 and H_2O adsorption, benzo[a]pyrene degradation, and atmospheric implications, J. Phys. Chem. A, 105, 4029–4041, doi:10.1021/jp004137n, 2001.

Powelson, M. H., Espelien, B. M., Hawkins, L. N., Galloway, M. M., and Haan, D. O. D.: Brown carbon formation by aqueous-phase carbonyl compound reactions with amines and ammonium sulfate, Environ. Sci. Technol., 48, 985–993, doi:10.1021/es4038325, 2014.

Qiu, C., Wang, L., Lal, V., Khalizov, A. F., and Zhang, R.: Heterogeneous reactions of alkylamines with ammonium sulfate and ammonium bisulfate, Environ. Sci Technol., 45, 4748–4755, doi:10.1021/es1043112, 2011.

Reis, S., Pinder, R. W., Zhang, M., Lijie, G., and Sutton, M. A.: Reactive nitrogen in atmospheric emission inventories, Atmos. Chem. Phys., 9, 7657–7677, doi:10.5194/acp-9-7657-2009, 2009.

Russell, L. M., Bahadur, R., and Ziemann, P. J.: Identifying organic aerosol sources by comparing functional group composition in chamber and atmospheric particles, P. Natl. Acad. Sci. USA, 108, 3516–3521, doi:10.1073/pnas.1006461108, 2011.

Saleh, R., Hennigan, C. J., McMeeking, G. R., Chuang, W. K., Robinson, E. S., Coe, H., Donahue, N. M., and Robinson, A. L.: Absorptivity of brown carbon in fresh and photo-chemically aged biomass-burning emissions, Atmos. Chem. Phys., 13, 7683–7693, doi:10.5194/acp-13-7683-2013, 2013.

Salma, I., Mészáros, T., Maenhaut, W., Vass, E., and Majer, Z.: Chirality and the origin of atmospheric humic-like substances, Atmos. Chem. Phys., 10, 1315–1327, doi:10.5194/acp-10-1315-2010, 2010.

Shilling, J. E., Chen, Q., King, S. M., Rosenoern, T., Kroll, J. H., Worsnop, D. R., DeCarlo, P. F., Aiken, A. C., Sueper, D., Jimenez, J. L., and Martin, S. T.: Loading-dependent elemental composition of α-pinene SOA particles, Atmos. Chem. Phys., 9, 771–782, doi:10.5194/acp-9-771-2009, 2009.

Souza, K. F., Carvalho, L. R. F., Allen, A. G., and Cardoso, A. A.: Diurnal and nocturnal measurements of PAH, nitro-PAH, and oxy-PAH compounds in atmospheric particulate matter of a sugar cane burning region, Atmos. Environ., 83, 193–201, doi:10.1016/j.atmosenv.2013.11.007, 2014.

Stocker, T. F., Qin, D., Plattner, G.-K., Tignor, M. M. B., Allen, S. K., Boschung, J., Nauels, A., Xia, Y., Bex, V., and Midgley, P. M.: Climate Change 2013. The Physical Science Basis,

Title Page

Abstract | Introduction

Conclusions | References

Tables | Figures

|◀ | ▶|

◀ | ▶

Back | Close

Full Screen / Esc

Printer-friendly Version

Interactive Discussion

Intergovernmental Panel on Climate Change, Cambridge University Press, Cambridge, UK and New York, NY, USA, 33, 2013.

Sun, Y.-L., Zhang, Q., Schwab, J. J., Demerjian, K. L., Chen, W.-N., Bae, M.-S., Hung, H.-M., Hogrefe, O., Frank, B., Rattigan, O. V., and Lin, Y.-C.: Characterization of the sources and processes of organic and inorganic aerosols in New York city with a high-resolution time-of-flight aerosol mass apectrometer, Atmos. Chem. Phys., 11, 1581–1602, doi:10.5194/acp-11-1581-2011, 2011.

Surratt, J. D., Kroll, J. H., Kleindienst, T. E., Edney, E. O., Claeys, M., Sorooshian, A., Ng, N. L., Offenberg, J. H., Lewandowski, M., Jaoui, M., Flagan, R. C., and Seinfeld, J. H.: Evidence for organosulfates in secondary organic aerosol, Environ. Sci. Technol., 41, 517–527, doi:10.1021/es062081q, 2006.

Swartz, E., Shi, Q., Davidovits, P., Jayne, J. T., Worsnop, D. R., and Kolb, C. E.: Uptake of gas-phase ammonia. 2. Uptake by sulfuric acid surfaces, J. Phys. Chem. A., 103, 8824–8833, doi:10.1021/jp991697h, 1999.

Trainic, M., Abo Riziq, A., Lavi, A., Flores, J. M., and Rudich, Y.: The optical, physical and chemical properties of the products of glyoxal uptake on ammonium sulfate seed aerosols, Atmos. Chem. Phys., 11, 9697–9707, doi:10.5194/acp-11-9697-2011, 2011.

Updyke, K. M., Nguyen, T. B., and Nizkorodov, S. A.: Formation of brown carbon via reactions of ammonia with secondary organic aerosols from biogenic and anthropogenic precursors, Atmos. Environ., 63, 22–31, doi:10.1016/j.atmosenv.2012.09.012, 2012.

Varutbangkul, V., Brechtel, F. J., Bahreini, R., Ng, N. L., Keywood, M. D., Kroll, J. H., Flagan, R. C., Seinfeld, J. H., Lee, A., and Goldstein, A. H.: Hygroscopicity of secondary organic aerosols formed by oxidation of cycloalkenes, monoterpenes, sesquiterpenes, and related compounds, Atmos. Chem. Phys., 6, 2367–2388, doi:10.5194/acp-6-2367-2006, 2006.

Wang, K., Ge, M., and Wang, W.: Kinetics of the gas-phase reactions of 5-hexen-2-one with OH and NO_3 radicals and O_3, Chem. Phys. Lett., 490, 29–33, doi:10.1016/j.cplett.2010.03.023, 2010.

Wang, X. F., Gao, S., Yang, X., Chen, H., Chen, J. M., Zhuang, G. S., Surratt, J. D., Chan, M. N., and Seinfeld, J. H.: Evidence for high molecular weight nitrogen-containing organic salts in urban aerosols, Environ. Sci. Technol., 44, 4441–4446, doi:10.1021/es1001117, 2010.

Widmann, J. F. and Davis, E. J.: Mathematical models of the uptake of $ClONO_2$ and other gases by atmospheric aerosols, J. Aerosol Sci., 28, 87–106, doi:10.1016/S0021-8502(96)00060-2, 1997.

Worsnop, D. R., Morris, J. W., Shi, Q., Davidovits, P., and Kolb, C. E.: A chemical kinetic model for reactive transformations of aerosol particles, Geophys. Res. Lett., 29, 1996, doi:10.1029/2002gl015542, 2002.

Wu, H. B., Chan, M. N., and Chan, C. K.: FTIR characterization of polymorphic transformation of ammonium nitrate, Aerosol Sci.Technol., 41, 581–588, doi:10.1080/02786820701272038, 2007.

Yu, G., Bayer, A. R., Galloway, M. M., Korshavn, K. J., Fry, C. G., and Keutsch, F. N.: Glyoxal in aqueous ammonium sulfate solutions: products, kinetics and hydration effects, Environ. Sci. Technol., 45, 6336–6342, doi:10.1021/es200989n, 2011.

Yu, J., Cocker III, D., Griffin, R., Flagan, R., and Seinfeld, J.: Gas-phase ozone oxidation of monoterpenes: gaseous and particulate products, J. Atmos. Chem., 34, 207–258, doi:10.1023/a:1006254930583, 1999.

Zarzana, K. J., De Haan, D. O., Freedman, M. A., Hasenkopf, C. A., and Tolbert, M. A.: Optical properties of the products of α-dicarbonyl and amine reactions in simulated cloud droplets, Environ. Sci. Technol., 46, 4845–4851, doi:10.1021/es2040152, 2012.

Zhang, D. and Zhang, R.: Ozonolysis of a-pinene and b-pinene: kinetics and mechanism, J. Chem. Phys., 122, 114308–114318, doi:10.1063/1.1862616, 2005.

Reactive uptake of ammonia to secondary organic aerosols

Y. Liu et al.

Title Page

Abstract | Introduction

Conclusions | References

Tables | Figures

|◀ | ▶|

◀ | ▶

Back | Close

Full Screen / Esc

Printer-friendly Version

Interactive Discussion

Reactive uptake of ammonia to secondary organic aerosols

Y. Liu et al.

Table 1. Initial gaseous and particle phase experimental conditions.

Exp. No[a].	VOC	c_{VOC} (ppbv)	c_{O_3} (ppbv)	c_{OH} (molecules cm^{-3})	c_{NH_3} (ppbv)	H_2SO_4/Na_2SO_4 (mol mol^{-1})	C_P (particles cm^{-3})	M_O^b (µg m^{-3})
P1	α-pinene	11.7	30.7	2.85×10^6	50.7	0.76	5863	11.2
P2	α-pinene	16.9	30.2	1.77×10^6	66.6	1.19	5627	16.4
P3	α-pinene	22.1	30.0	3.41×10^6	34.1	2.12	5377	23.5
P4	α-pinene	13.6	31.2	2.81×10^6	40.6	1.71	4761	13.6
P5	α-pinene	13.3	33.4	2.22×10^6	49.7		3836	5.8
P6	α-pinene	13.6	33.3	1.57×10^6	40.8	1.68	5276	13.6
B7	–	0	31.8	–	44.0	1.68	4656	0.4
P8	α-pinene	11.9	33.1	1.87×10^6	34.1	1.95	4632	12.8
P9	α-pinene	11.2	31.0	2.18×10^6	42.6	1.95	5554	10.4
P10	α-pinene	11.3	31.0	3.01×10^6	56.6	1.95	5437	15.4
P11	α-pinene	11.2	31.0	2.41×10^6	63.9	1.95	5464	14.6
P12	α-pinene	12.8	30.9	3.47×10^6	101.5	1.95	5495	20.6
P13	α-pinene	10.4	31.2	3.41×10^6	75.1	1.95	5402	16.6
P14	α-pinene	10.9	29.2	3.49×10^6	61.9	1.95	5809	15.6
M15	m-xylene	21.6	–	1.74×10^6	49.4	1.95	4910	6.4
M16	m-xylene	25.0	–	1.82×10^6	66.2	1.95	4966	6.8
M17	m-xylene	23.3	–	1.78×10^6	86.2	1.95	4948	6.0
M18	m-xylene	21.1	–	1.40×10^6	97.9	1.95	4612	5.4
M19	m-xylene	22.1	–	1.93×10^6	104.4	1.95	4918	5.8
M20	m-xylene	19.7	–	1.31×10^6	125.7	1.95	5248	5.6

[a] P, B and M represent. α-pinene, blank and m-xylene, respectively. Experiments performed at RH = 50 ± 1 %; T = 295 ± 2 K.
[b] Organics after 6 h of exposure.

Table 2. Contribution of NOC to SOA and total nitrogen containing mass.

Exp. No[a].	VOC	SOA yield (%)	$(\gamma_{t, ini})$[b]	N / C	$C_xH_yN_n/T_{NOC}^c$ (%)	$C_xH_yON_n/T_{NOC}^c$ (%)	$C_xH_yO_2N_n/T_{NOC}^c$ (%)	NO_x/T_{NOC}^c (%)	NOC/TN (%)[d]	N_{NOC}/N_{TN}^d (%)[e]	T_{NOC}^c/SOA (%)[f]
P1	α-pinene	22.1	$1.64 \pm 0.07 \times 10^{-3}$	1.3×10^{-2}	15.1	11.8	11.1	62.0	18.5	8.7	11.0
P2	α-pinene	23.3	$2.00 \pm 0.58 \times 10^{-3}$	1.3×10^{-2}	19.9	14.1	18.1	47.9	17.3	7.3	9.3
P3	α-pinene	26.0	$5.47 \pm 0.23 \times 10^{-3}$	1.5×10^{-2}	30.0	19.8	15.5	34.6	18.5	7.7	8.2
P4	α-pinene	26.6	$5.21 \pm 0.16 \times 10^{-3}$	2.3×10^{-2}	35.8	19.3	15.5	29.3	18.6	8.2	12.2
P5	α-pinene	11.6	$1.23 \pm 0.04 \times 10^{-3}$	2.2×10^{-2}	40.8	24.6	16.9	17.7	40.1	19.2	9.0
P6	α-pinene	24.4	$3.05 \pm 0.11 \times 10^{-3}$	1.8×10^{-2}	33.5	17.0	12.2	37.2	16.3	6.9	10.2
B7	–	–	–	–	–	–	–	–	–	–	–
P8	α-pinene	24.8	$4.02 \pm 0.18 \times 10^{-3}$	2.1×10^{-2}	39.8	22.0	13.2	25.0	14.3	5.7	9.7
P9	α-pinene	20.8	$2.61 \pm 0.22 \times 10^{-3}$	1.8×10^{-2}	32.3	19.3	20.8	27.7	12.2	4.7	9.2
P10	α-pinene	29.4	$1.78 \pm 0.07 \times 10^{-3}$	1.5×10^{-2}	27.7	21.7	18.9	31.7	11.6	4.5	7.8
P11	α-pinene	28.0	$1.64 \pm 0.10 \times 10^{-3}$	1.4×10^{-2}	29.4	21.8	15.4	33.4	10.1	3.9	7.1
P12	α-pinene	32.0	$1.62 \pm 0.09 \times 10^{-3}$	1.5×10^{-2}	42.4	22.4	18.1	17.1	11.8	5.3	7.3
P13	α-pinene	31.8	$1.24 \pm 0.08 \times 10^{-3}$	1.1×10^{-2}	29.5	17.3	19.1	34.1	11.5	4.5	6.2
P14	α-pinene	28.6	$1.53 \pm 0.06 \times 10^{-3}$	1.4×10^{-2}	30.7	19.0	16.2	34.1	11.9	4.7	7.1
M15	m-xylene	12.6	$1.52 \pm 0.03 \times 10^{-2}$	6.4×10^{-2}	34.3	15.7	4.5	45.6	23.1	10.0	28.9
M16	m-xylene	9.8	$8.21 \pm 0.30 \times 10^{-3}$	5.6×10^{-2}	27.6	16.1	7.6	48.8	20.4	8.5	28.2
M17	m-xylene	9.8	$6.74 \pm 0.19 \times 10^{-3}$	6.6×10^{-2}	32.7	17.6	3.6	46.1	20	8.6	30.1
M18	m-xylene	11.6	$4.00 \pm 0.11 \times 10^{-3}$	7.6×10^{-2}	32.1	15.3	5.4	47.2	20.4	14	35.9
M19	m-xylene	9.4	$3.98 \pm 0.10 \times 10^{-3}$	5.1×10^{-2}	24.4	14.8	6.2	54.6	16.3	11.8	27.5
M20	m-xylene	12.8	$4.10 \pm 0.13 \times 10^{-3}$	7.9×10^{-2}	32.8	15.1	5.0	47.1	21.4	14.8	38.1
Mean ± σ			$4.0 \pm 3.3 \times 10^{-3}$		31.1 ± 6.7	18.1 ± 3.4	12.8 ± 5.7	38.0 ± 12.1	17.6 ± 6.7	8.4 ± 4.1	16.0 ± 11

[a] P, B and M represent α-pinene, blank and m-xylene, respectively.
[b] γ leading to T_{NOC} derived excluding NH_x fragments.
[c] After 6 h of exposure where $T_{NOC} = C_xH_yN_n + C_xH_yON_n + C_xH_yO_2N_n + NO_x$.
[d] Where TN includes all nitrogen containing mass, including ammonium (TN $= C_xH_yN_n + C_xH_yON_n + C_xH_yO_2N_n + NO_x + NH_x$).
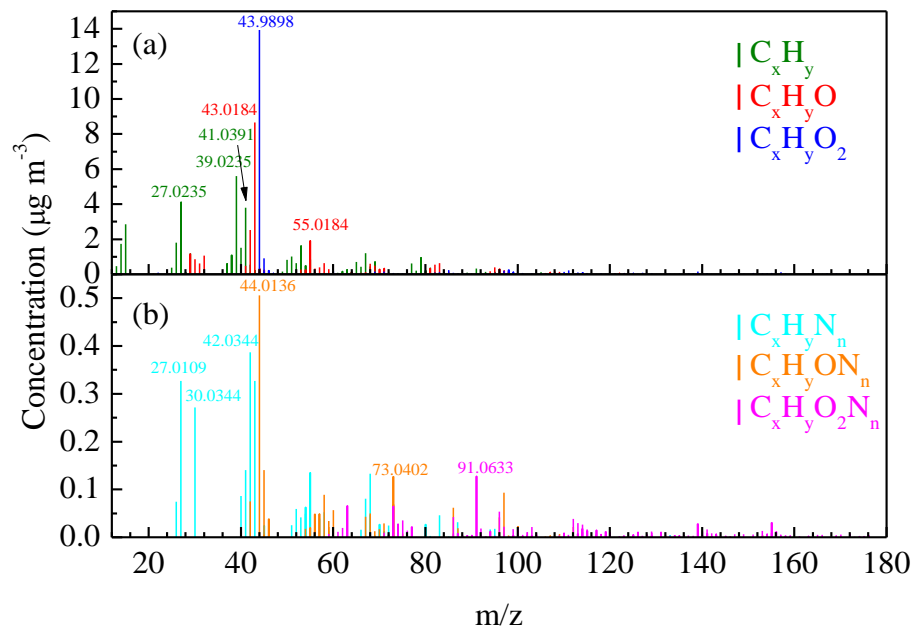[e] Values given on a N atom/N atom mass basis.
[f] Ratio on a mass/mass basis.

Figure 1. Typical HR-ToF-AMS spectra of **(a)** non-N-containing fragments and **(b)** N-containing fragments in SOA formed by O_3 oxidation of α-pinene in the presence of 40.8 ppbv NH_3 (Exp. P5).

Discussion Paper | Discussion Paper | Discussion Paper | Discussion Paper

ACPD

15, 17449–17490, 2015

Reactive uptake of ammonia to secondary organic aerosols

Y. Liu et al.

Title Page

Abstract | Introduction

Conclusions | References

Tables | Figures

|◄ | ►|

◄ | ►

Back | Close

Full Screen / Esc

Printer-friendly Version

Interactive Discussion
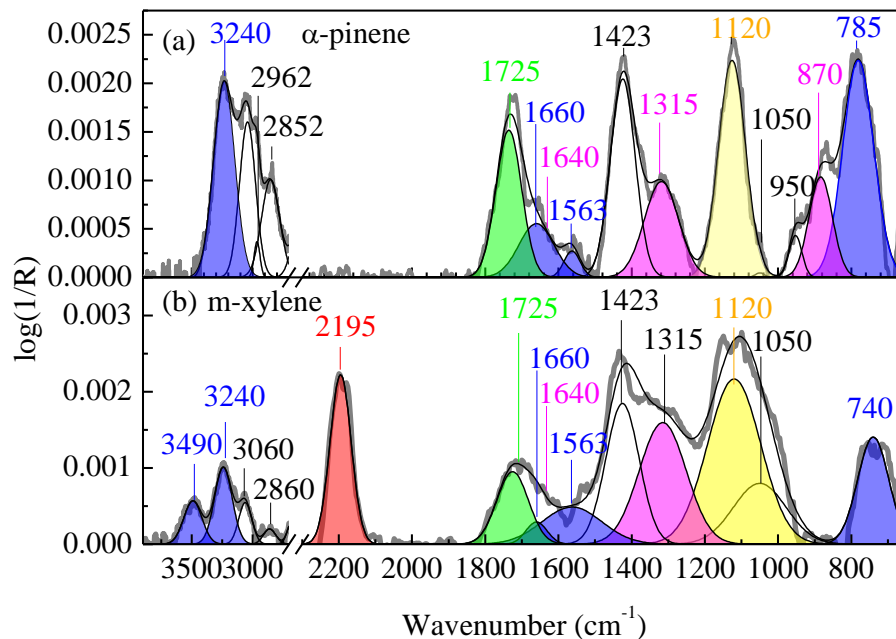
Figure 2. Infrared spectra for SOA from **(a)** ozonolysis of α-pinene (Exp. P11) and **(b)** OH oxidation of m-xylene (Exp. M15) in the presence of NH$_3$. R is the abbreviation for reflectance in DRIFTS mode.
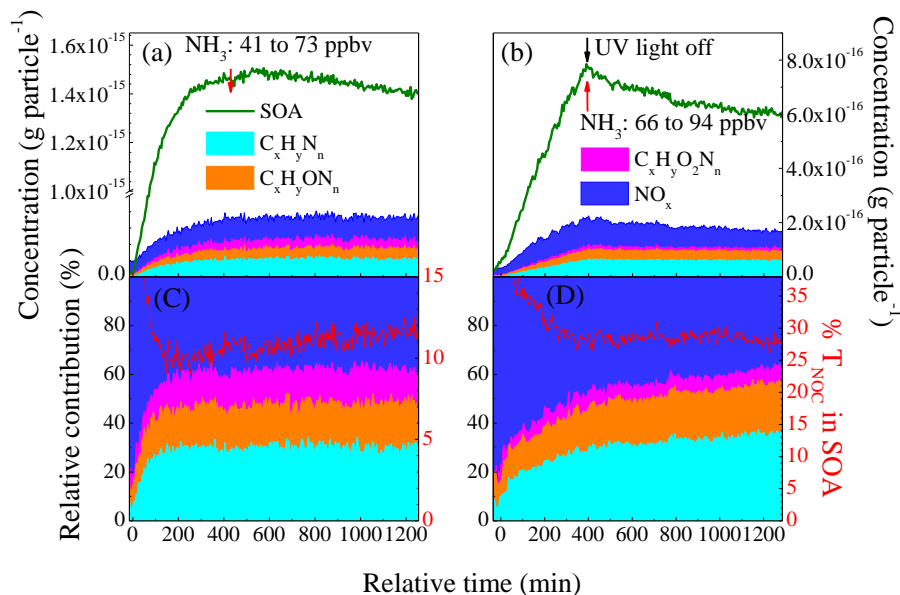
Figure 3. Concentration changes for N-containing fragments and SOA for **(a)** ozonolysis of α-pinene (Exp. P6) and **(b)** OH oxidation of m-xylene (Exp. M16), respectively; the relative fraction of each species to total NOC mass ($T_{\mathrm{NOC}} = C_xH_yN + C_xH_yON + C_xH_yO_2N + NO_x$) and T_{NOC} to SOA fraction for **(c)** ozonolysis of α-pinene and **(d)** OH oxidation of m-xylene, respectively.
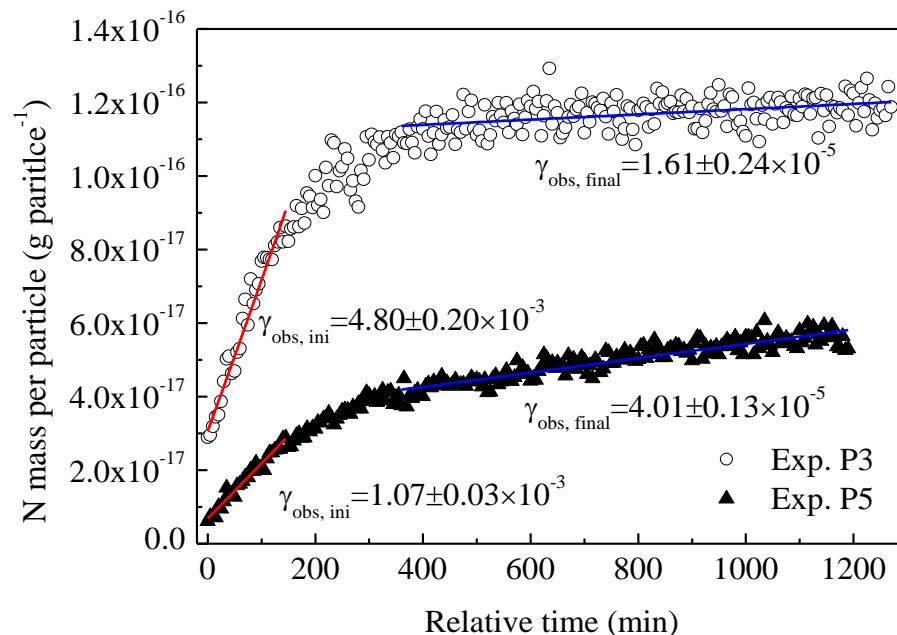
Figure 4. Fitting of mass changes (Exp. P3 and P5) to derive uptake coefficients for NH_3 leading to T_{NOC}. The red and blue lines represent the predicted values by the uptake model at the initial (from 0 to 150 min) and the final stages of the experiment (from 400 to 1250 min), respectively.
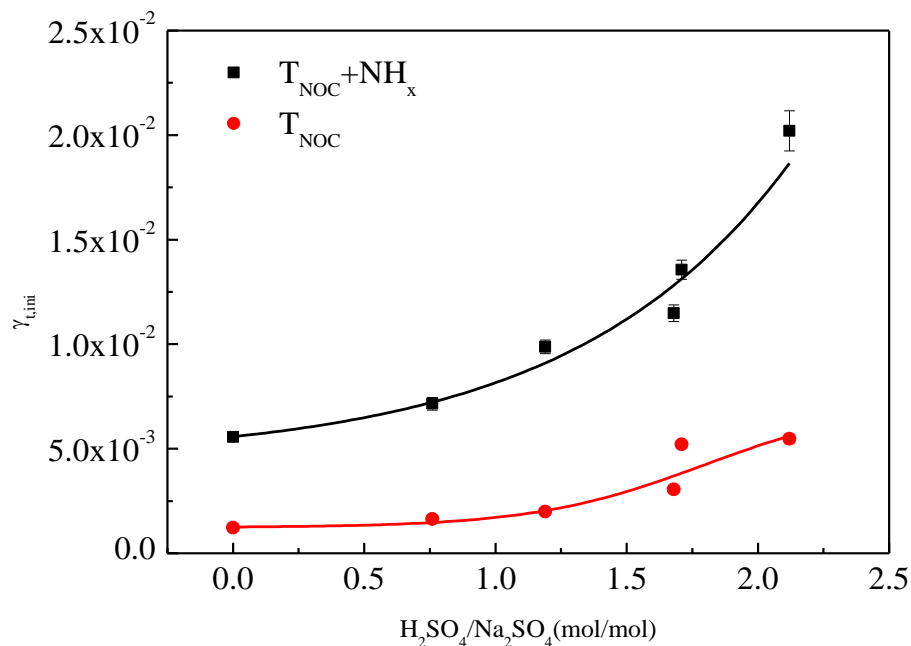
Figure 5. Relationship between the $\gamma_{t,ini}$ and particle-phase acidity when including (black) and excluding (red) NH_x in the determination of γ. The error bars are derived from the uncertainties of the uptake model parameters.
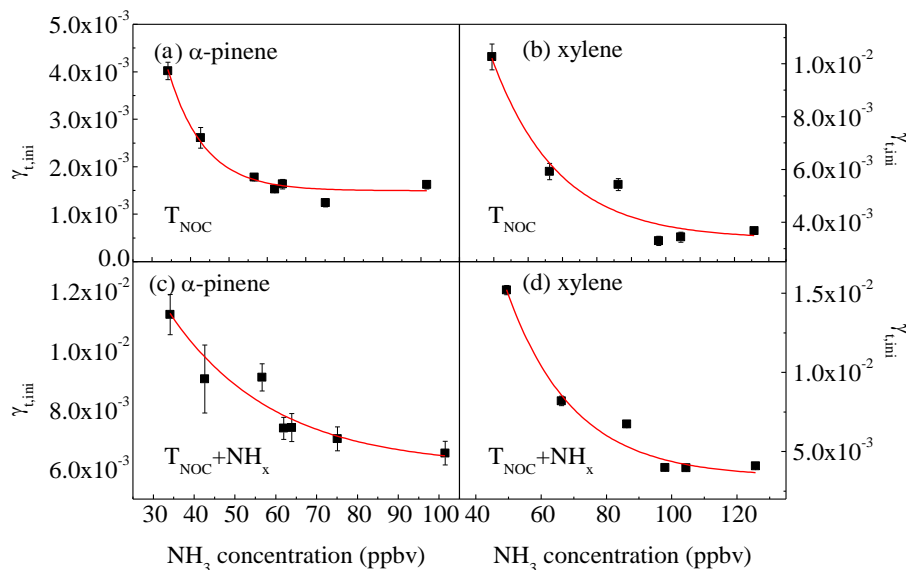
Figure 6. Diffusion corrected uptake coefficient of NH_3 to form NOC species on SOA from O_3 oxidation of α-pinene **(a)** and OH oxidation of m-xylene **(b)**, as a function of NH_3 exposure (at fixed H_2SO_4/Na_2SO_4 ratio; 1.95 mol mol^{-1}). This relationship is also shown for uptake coefficients derived including the NH_x fragments **(b)** and **(c)**. The error bars depict 1σ.
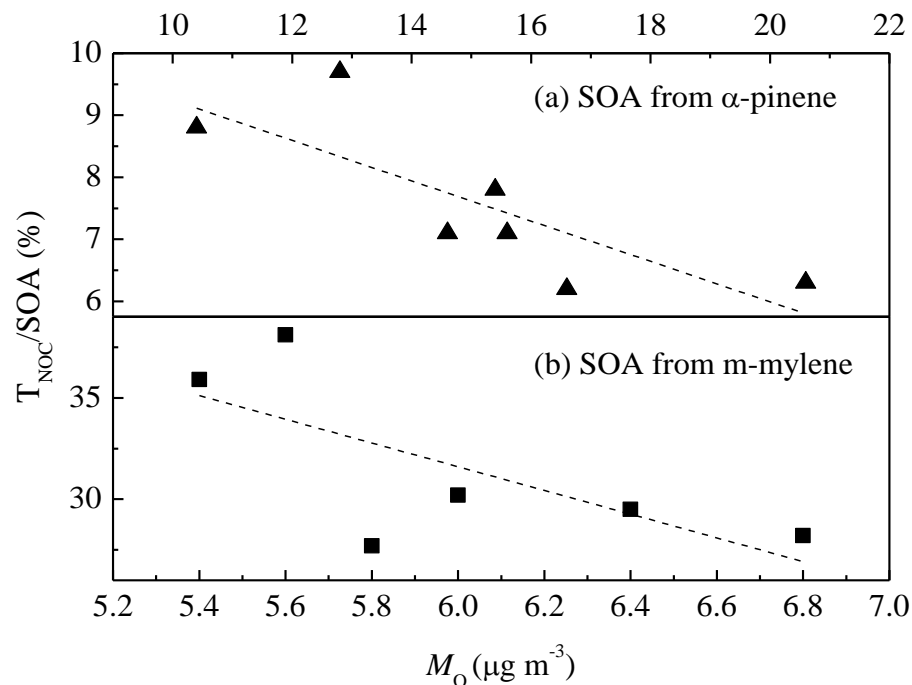
Figure 7. Relative contribution of NOC to the total SOA (T_{NOC}/SOA) as a function of organic mass loading for α-pinene and m-xylene experiments at constant particle acidity (H_2SO_4/Na_2SO_4: 1.95).